PROCEEDINGS

MMM 2008

Fourth International Conference

MULTISCALE MATERIALS MODELING

OCTOBER 27-31, 2008 ▪ TALLAHASSEE, FLORIDA, USA

Tackling Materials Complexities via Computational Science

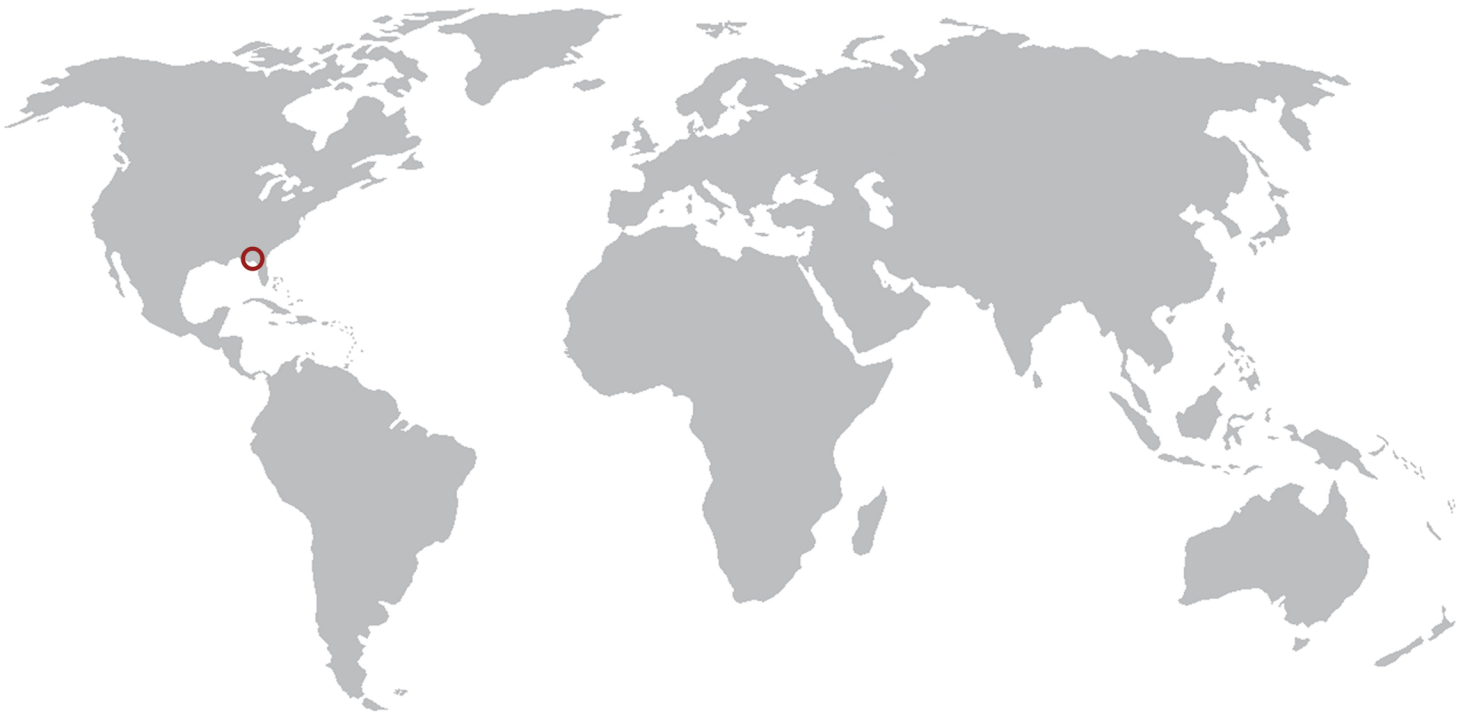

Hosted by the Department of Scientific Computing and Florida State University

DEPARTMENT OF Scientific COMPUTING

FLORIDA STATE UNIVERSITY 1851 VIRES ARTES MORES

Proceedings of

MMM 2008

Fourth International Conference

MULTISCALE MATERIALS MODELING

OCTOBER 27-31, 2008 ▪ TALLAHASSEE, FLORIDA, USA

Anter El-Azab
Editor

Organized and Hosted by
The Department of Scientific Computing and
Florida State University

DEPARTMENT OF Scientific COMPUTING

Papers published in this volume constitute the proceedings of the Fourth International Conference on Multiscale Materials Modeling (MMM-2008). Papers were selected by the program committee for oral or poster presentation. They are published as submitted, in the interest of timely dissemination.

ISBN 978-0-615-24781-6

Copyright © 2008
Department of Scientific Computing
Florida State University
400 Dirac Science Library
P.O. Box 3064120
Tallahassee, FL 32306-4120

All rights reserved. No part of this publication may be translated, reproduced, stored in a retrieval system, or transmitted in any form or by any means, electronic, mechanical, photocopying, recording or otherwise, without the written permission of the publisher.

Printed in the United States of America

Forward

The field of multiscale modeling of materials promotes the development of predictive materials research tools that can be used to understand the structure and properties of materials at all scales and help us process materials with novel properties. By its very nature, this field transcends the boundaries between materials science, mechanics, and physics and chemistry of materials. The increasing interest in this field by mathematicians and computational scientists is creating opportunities for solving computational problems in the field with unprecedented levels of rigor and accuracy. Because it is a part of the wider field of materials science, multiscale materials research is intimately linked with experiments and, together, these methodologies serve the dual role of enhancing our fundamental understanding of materials and enabling materials design for improved performance.

The increasing role of multiscale modeling in materials research motivated the materials science community to start the Multiscale Materials Modeling (MMM) Conference series in 2002, with the goal of promoting new concepts in the field and fostering technical exchange within the community. Three successful conferences in this series have been already held:

- The First International Conference on Multiscale Materials Modeling (MMM-2002) at Queen Mary University of London, UK, June 17-20, 2002,
- Second International Conference on Multiscale Materials Modeling (MMM-2004) at the University of California in Los Angeles, USA, October 11-15, 2004, and
- Third International Conference on Multiscale Materials Modeling (MMM-2006) at the University of Freiburg, Germany, September 18-22, 2006.

The Fourth International Conference on Multiscale Materials Modeling (MMM-2008) held at Florida State University comes at a time when the wider computational science field is shaping up and the synergy between the materials modeling community and computational scientists and mathematicians is becoming significant. The overarching theme of the MMM-2008 conference is thus chosen to be "*Tackling Materials Complexities via Computational Science*," a theme that highlights the connection between multiscale materials modeling and the wider computational science field and also reflects the level of maturity that the field of multiscale materials research has come to. The conference covers topics ranging from basic multiscale modeling principles all the way to computational materials design. Nine symposia have been organized, which span the following topical areas:

- Mathematical basis for multiscale modeling of materials
- Statistical frameworks for multiscale materials modeling
- Mechanics of materials across time and length scales
- Multiscale modeling of microstructure evolution in materials
- Defects in materials
- Computational materials design based on multiscale and multi-level modeling principles

- Multiscale modeling of radiation effects in materials and materials response under extreme conditions
- Multiscale modeling of bio and soft matter systems

The first five topical areas are intended to cover the theoretical and computational basis for multiscale modeling of materials. The sixth topical area is intended to demonstrate the technological importance and industrial potential of multiscale materials modeling techniques, and to stimulate academia-laboratory-industrial interactions. The last two topical areas highly overlap with the earlier ones, yet they bring to the conference distinct materials phenomena and modeling problems and approaches with unique multiscale modeling aspects.

This conference would not have been possible without the help of many individuals both at Florida State University and around the world. Of those, I would like to thank the organizing team of MMM-2006, especially Professor Peter Gumbsch, for sharing their experience and much organizational material with us. I also thank all members of the International Advisory Board for their support and insight during the early organizational phase of the conference, and the members of the International Organizing Committee for the hard work in pulling the conference symposia together and for putting up with the many organization-related requests. Thanks are due to Professor Max Gunzburger, Chairman of the Department of Scientific Computing (formerly School of Computational Science) and to Florida State University for making available financial, logistical and administrative support without which the MMM-2008 would not have been possible. The following local organizing team members have devoted significant effort and time to MMM-2008 organization: Bill Burgess, Anne Johnson, Michele Locke, Jim Wilgenbusch, Christopher Cprek and Michael McDonald. Thanks are also due to my students Srujan Rokkam, Steve Henke, Jie Deng, Santosh Dubey, Mamdouh Mohamed and Jennifer Murray for helping with various organizational tasks. Special thanks are due to Bill Burgess and Srujan Rokkam for their hard work on the preparation of the proceedings volume and conference program.

I would like to thank the MMM-2008 sponsors: Lawrence Livermore National Laboratory (Dr. Tomas Diaz de la Rubia), Oak Ridge National Laboratory (Dr. Steve Zinkle) and Army Research Office (Drs. Bruce LaMattina and A.M. Rajendran) for the generous financial support, and thank TMS (Dr. Todd Osman) for the sponsorship of MMM-2008 and for advertising the conference through the TMS website and other TMS forums.

I would also like to thank all plenary speakers and panelists for accepting our invitation to give plenary lectures and/or serve on the conference panels. Lastly, I would like to thank the session chairs for managing the conference sessions.

Anter El-Azab
Conference Chair

International Advisory Board

Dr. Tomas Diaz de la Rubia	LLNL, USA
Prof. Peter Gumbsch	Fraunhofer Institute IWM, Freiburg, Germany
Dr. A.M. Rajendran	ARO, USA
Dr. Steve Zinkle	ORNL, USA
Prof. Anter El-Azab	FSU, USA
Prof. Michael Zaiser	Edinburgh, UK
Prof. Xiao Guo	Queens, London, UK
Prof. Shuichi Iwata	University of Tokyo, Japan
Prof. Jan Kratochvil	CTU, Prague, Czech Republic
Prof. Nasr Ghoniem (Chair)	UCLA, USA
Dr. Ladislas Kubin	ONERA-LEM, France
Prof. Shaker Meguid	Toronto, Canada
Prof. Alan Needleman	Brown, USA
Prof. Michael Ortiz	Caltech, USA
Prof. David Pettifor	Oxford, UK
Prof. Robert Phillips	Caltech, USA
Prof. Dierk Raabe	Max Planck Institute, Duesseldorf, Germany
Prof. Yoji Shibutani	Osaka University, Japan
Prof. Subra Suresh	MIT, Massachusetts USA
Prof. Yoshihiro Tomita	Kobe University, Japan
Prof. Erik Van der Giessen	University of Groningen, The Netherlands
Dr. Dieter Wolf	INL, USA
Prof. Sidney Yip	MIT, USA
Prof. David Bacon	Liverpool, UK
Dr. Michael Baskes	LANL, USA
Prof. Esteban Busso	Ecole des Mines, France
Prof. Timothy Cale	RPI, New York, USA
Dr. Moe Khaleel	PNNL, USA
Prof. David Srolovitz	Yeshiva, USA
Prof. Emily Carter	Priceton University, USA
Dr. Dennis Dimiduk	AFRL, USA
Prof. Rich Le Sar	Iowa State University, USA

International Organizing Committee

Weinan E	Princeton University, USA
Max Gunzburger	Florida State University, USA
Mitchell Luskin	University of Minnesota, USA
Rich Lehoucq	Sandia National Laboratories, USA
A.M. Rajendran	U.S. Army Research Office, USA
Stefano Zapperi	University of Rome, Italy
M.-Carmen Miguel	University of Barcelona, Spain
Mikko Alava	Helsinki University of Technology, Finland
Istevan Groma	Eötvös University, Hungary
Tom Arsenlis	Lawrence Livermore National Laboratory, USA
Peter Chung	Army Research Laboratory, USA

Marc Geers	Eindhoven University of Technology, The Netherlands
Yoji Shibutani	Osaka University, Japan
Dieter Wolf	Idaho National Laboratory, USA
Jeff Simmons	Air Force Research Laboratory, USA
Simon Phillpot	University of Florida, USA
Anter El-Azab (Chair)	Florida State University, USA
Daniel Weygand	University of Karlsruhe (TH), Germany
Zi-Kui Liu	Pennsylvania State University, USA
Hamid Garmestani	Georgia Institute of Technology, USA
Moe Khaleel	Pcific Northwest National Laboratory, USA
Mei Li	Ford Motor Company, USA
Fie Gao	Pacific Northwest National Laboratory, USA
Roger Stoller	Oak Ridge National Laboratory, USA
Pascal Bellon	University of Illinois, Urbana-Champaign, USA
Syo Matsumura	Kyushu University, Japan
Jeffery G. Saven	University of Pennsylvania, USA
Wei Yang	Florida State University, USA
T.P. Straatsma	Pacific Northwest National Laboratory, USA
L.P. Kubin	CNRS-ONERA, France
S.J. Zinkle	Oak Ridge National Laboratory, USA
Jaafar El-Awady	University of California, Los Angeles, USA
Shahram Sharafat	University of California, Los Angeles, USA
Hanchen Huang	Rensselaer Polytechnic Institute, USA
Yury N. Osetskiy	Oak Ridge National Laboratory, USA
Ron O. Scattergood	North Carolina State University, USA
Anna M. Serra	Universitat Politecnica de Catalunya, Spain

Local Organizing Committee (Florida State University, USA)

Prof. Anter El-Azab (Chair)
Prof. Max Gunzburger (Co-Chair)
Anne Johnson (Public relations and marketing)
Bill Burgers (Graphics and publications)
Srujan Rokkam (Proceedings and printing)
Michael McDonald (Webmaster)
Michele Locke (Finances)

Sponsors

Special thanks to the following sponsors:

- The Army Research Office
- Lawrence Livermore National Laboratory
- Oak Ridge National Laboratory

for their generous financial support, and to

- The Minerals, Metals & Materials Society (TMS)

for the sponsoring and advertising the conference through the TMS website.

Contents

Symposium 7

Symposium 7

Computational modeling of biological and soft condensed matter systems

A Systematic Approach for Coarse-graining Biomolecular and Soft Matter Systems

Gregory A. Voth

Center for Biophysical Modeling and Simulation and Department of Chemistry, University of Utah, 315 S. 1400 E., Rm. 2020, Salt Lake City, Utah 84112-0850
(E-mail: voth@chem.utah.edu)

ABSTRACT

A multiscale theoretical and computational methodology will be presented for characterizing biomolecular and soft matter systems across multiple length- and time-scales. The approach provides a connection between all-atom molecular dynamics, mesoscopic models, and near continuum-scale mechanics. At the heart of the methodology is the multiscale coarse-graining (MS-CG) method for systematically deriving coarse-grained models from atomistic-scale forces. Applications will be given for membranes, peptides, and proteins. Recent advances for coarse-graining large protein complexes and membrane proteins will also be described if time allows.

Characterizing and Mimicking Marine Biological Materials: Recent Experimental Results and Current Needs for Modeling

Cristina Matos, James White, Lauren Hight, Jeremy Burkett, Jessica Wojtas, Joshua Cloud, Jonathan Wilker

Department of Chemistry, Purdue University, West Lafayette, IN 47907, USA (E-mail: wilker@purdue.edu)

ABSTRACT

Mussels and barnacles are examples of the many marine organisms that affix themselves to surfaces by production of adhesive and cement materials. Our laboratory is working to characterize these biological materials, design synthetic mimics, and develop applications. Mussel adhesive is comprised of a mixture of proteins containing the unusual DOPA (3,4-dihydroxyphenylalanine) amino acid. Barnacle cement is also protein-based, but less is known about the specific components. Once applied to a surface, these proteins are cross-linked to yield the final, cured material. We have begun our experimental efforts with characterization studies. Experiments involve work with the live animals, extracted protein, and model peptides. Recent results indicate that iron is the key reagent used by mussels to initiate the cross-linking process for adhesive formation. More recently we have developed a new class of synthetic polymers mimicking the adhesive properties of these proteins. Our presentation will begin with experimental findings and then highlight research areas in need of modeling insights. Such modeling efforts may help to understand these biological materials as well as aid the design of new bioinspired materials.

A Multi-Scale Model for Kinetics of Formation and Disintegration of Spherical Micelles

Gunjan Mohan, Dmitry Kopelevich

Department of Chemical Engineering, University of Florida, Gainesville, FL, USA
(E-mails: gmohan@che.ufl.edu, dkopelevich@che.ufl.edu)

ABSTRACT

Dynamics of self-assembly and structural transitions in amphiphilic systems play an important role in numerous processes, ranging from production of nanostructured materials to transport in biological cells. Theoretical and computational modeling of these processes is extremely challenging due to the large span of length- and time-scales involved. In this talk, we discuss development of a multi-scale model for formation and disintegration of non-ionic and ionic spherical micelles. The study is performed under the assumption that the dominant mechanism of micelle formation (disintegration) is a stepwise addition (removal) of single monomers to (from) a surfactant aggregate. Different scales of these processes are investigated using a combination of coarse-grained molecular dynamics simulations, analytical and numerical solution of stochastic differential equations, and a numerical solution of kinetic equations. The removal of a surfactant from an aggregate is modeled by a Langevin equation for a single reaction coordinate, the distance between the centers of mass of the surfactant and the aggregate, with parameters obtained from a series of constrained molecular dynamics simulations. We demonstrate that the reverse process of addition of a surfactant molecule to an aggregate involves at least two additional degrees of freedom, orientation of the surfactant molecule and micellar microstructure. Formation of the ionic micelles involves one more degree of freedom which describes collective dynamics of the charges in the system. Time-scales of the additional degrees of freedom are comparable with the timescale of the monomer addition to a micelle and hence these degrees of freedom play an active role in the monomer addition process. We demonstrate that neglecting their contribution leads to qualitative discrepancies in predicted surfactant addition rates and propose a stochastic model for the monomer addition which takes the additional degrees of freedom into account. The model parameters are extracted from molecular dynamics simulations and the surfactant addition rates are determined from Brownian dynamics simulations of this model. The obtained addition and removal rates are then incorporated into the kinetic model of micellar formation and disintegration. It is expected that insights gained in the course of development of the multi-scale model for this relatively simple self-assembly process will aid in the development of models for dynamics of more complex amphiphilic systems.

A Model of Hybrid Simulations of MD and CFD

Shugo Yasuda[1,2] and Ryoichi Yamamoto[1,2]

[1] Department of Chemical Engineering, Kyoto University, Kyoto 615-8510, Japan
[2] CREST, Japan Science and Technology Agency, Kawaguchi 332-0012, Japan
(E-mail: yasuda@cheme.kyoto-u.ac.jp)

ABSTRACT

The idea of multi-scale hybrid simulation is expected to be very useful for overcoming several difficult problems remain unsolved in frontiers of computational science in general. A striking example is the case of hydrodynamics of complex fluids or soft matters, for most of which no reliable constitutive relation is known explicitly. Our strategy to overcome this problem is very straightforward. We are developing a multi-scale hybrid method which combines computational fluid dynamics (CFD) as a fluid solver and molecular dynamics (MD) as a direct generator of constitutive relations in a consistent way. The numerical algorithm is rather simple. We perform usual lattice-mesh based simulations for CFD level, but each lattice is associated with a small MD cell which generates a "local stress" according to a "local flow field" given from CFD instead of using any constitutive functions at CFD level. MD simulations thus have to be performed at all lattices and at every time steps of CFD. The basic ideas to implement the present method were put forward earlier by W. E and his collaborators.[1] We carried out hybrid simulations for some elemental flow problems involving simple Lennard-Jones liquids and compared the results with those obtained by usual CFD with a Newtonian constitutive relation in order to examine the validity of the hybrid simulation method. It is demonstrated that the hybrid simulations successfully reproduce the correct flow behavior obtained from usual CFD as long as the mesh size Δx and the time-step Δt of CFD are not too large compared to the system size l_{MD} and the sampling duration t_{MD} of MD simulations performed at each time step of the CFD. Otherwise, the simulations are affected by large fluctuations due to poor statistical averages taken in the MD part. Properties of the fluctuations are also investigated in detail by comparing with the results obtained by the fluctuating hydrodynamics.[2] We will also demonstrate some tentative results for complex fluids.

[1] W. E, B. Engquist, X. Li, W. Ren and E. Vanden-Eijnden, "Heterogeneous multiscale methods: a review", Commun. Comput. Phys. **2**, 367 (2007).
[2] S. Yasuda and R. Yamamoto, "A model for hybrid simulations of molecular dynamics and CFD", Phys. Fluids (submitted).

Coarse Grain Modeling of Piezoelectric Polyimide Copolymers

Arnab Chakrabarty, Tahir Cagin

Department of Chemical Engineering,
Texas A&M University, College Station, Texas 77843-3122.
(E-mail: cagin@che.tamu.edu)

ABSTRACT

In this paper, we present development of a coarse grain bead model for piezoelectric polyimide copolymers for large-scale simulations of thermal, mechanical, electrical properties. We also demonstrate the application of this model on dynamic loading simulations of these polymers.

1. Introduction

Classical molecular dynamics (MD) is a useful method in studying materials at the molecular level. However, MD is inherently limited in time and length scales if no compromise is made at the molecular level details. Unfortunately the timescale at which most of the phenomena occurs in a polymer, due to its slow segmental movements is rather large relative to the accessible timescales of a typical MD simulation. On the other hand, in order to have realistic estimates and reliable conclusions especially for an amorphous polymer, relatively larger system than what a typical MD simulation can address, is desired. Achievable time scales are dictated by the high frequency modes arising from the molecular bonds. Hence leading to coverage of a smaller domain in phase space using classical MD. Coarse Grain (CG) representation, a step next to MD in multi-scale modeling approach, one can eliminate these fast modes systematically. This route has been employed earlier[1-8] where the finer details of the system are averaged out in order to simulate larger size models for longer periods of time through developing a low-resolution model.

In our present work we have developed CG parameters for an amorphous, aromatic, piezoelectric polyimide exclusively based on our atomistic level simulation results and have made an attempt to describe the system by a CG model without compromising material specificity. This, in turn led to a gain in the order of hundreds in terms of computational time.

2. Coarse Grain Model and Parameterization

Coarsening refers to lumping a set of atoms into a single super-atom. The use of coarsened model enables accessing the larger timescale and length scale phenomena in polymers[9-12]. Another use of CG models is to get an equilibrated structure faster through mapping and reverse mapping from atomistic to coarsened model [1,13,14]. Critical issues here are the mapping techniques [13,14] and a systematic approach in building a CG model [4,15,16]. Various approaches

such as dissipative particle dynamics[17,18], Boltzmann inversion technique[14,19], force matching method[20], fitting energy distribution[2,21] have been used. Successes in CG modelling have been demonstrated through applications on biological systems [8,9,22-24], polymers [3,5,14,25,26] dendrimers [3,27] and liquid state systems [28,29]. However, we must note that coarsening is specific to a system and hence may not be transferable to different systems.

2.1 Coarse Grain Parameters

Figure 1: Coarsening an atomistic model

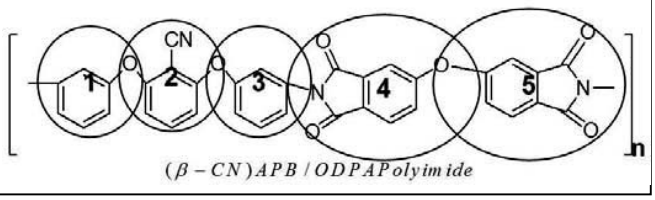

Based on the structure and piezoelectric property, the system was coarsened from 62-atoms per monomer to a 5-interaction center per monomer polymer system as illustrated in Figure 1.

The interactions of this system were described by the following potential energy expression:

$E = E_b + E_{angle} + E_{vdw} + E_{coul}$,

We have estimated the parameters for the above mentioned energy terms as follows:

E_b : The "bond" stretch energy was described through a harmonic function, $E_b = \frac{1}{2} k_b (r - r_0)^2$

k_b is the force constant and r_0 is the equilibrium bond length. The force constant and equilibrium bond length were determined from all atom MD simulations. E_{angle}: Parameters for angle bending energy were estimated in a similar fashion.

E_{vdw}: Isolated groups of atoms defining a bead were taken and theor pairwise interaction energies were calculated by varying distance and orientation. The charges on the individual atoms were zeroed out to isolate the effect of the van-der-Waals interaction. The average energy obtained was fitted to a Morse potential (Equation 4) to estimate the parameters.

$$E_{VDW} = D\left\{\left(e^{-0.5\alpha\left(\frac{r_{ij}}{r_0}-1\right)}\right)^2 - 2\left(e^{-0.5\alpha\left(\frac{r_{ij}}{r_0}-1\right)}\right)\right\}$$

The parameters estimated were taken as the initial set of parameters and were further refined to meet atomistic density and stiffness of the system through bulk phase calculations.

E_{coul}: The electrostatic interaction was estimated from monopole interaction. The summation of charges on each set of atoms defining a group was assigned to the bead.

3. Physical and Chain Properties of Models

Various properties of the coarsened polymer model were estimated and compared with its atomistic counterpart to present validity of our approach, see Tables 1 and 2.

Table 1. Comparison of physical properties obtained from atomistic and coarse grain models. (Notation M_N: A Polymer model with M chains and N monomers per chain). Calculations for some large scale atomistic models were not performed denoted as N/A.

Sample	Beads	Atoms	ρ gm/cc		Dielectric constant (Kirkwood-Frohlich Method)	
			CG	MD	MD	CG
10_30	1500	18620	1.26	1.28	3.3	1.81
20_30	3000	37240	1.25	1.29	3.03	4.78
15_40	3000	37230	1.24	1.26	2.63	2.32
30_40	6000	74460	1.26	1.26	3.39	2.28
40_40	8000	99280	1.24	1.29	2.88	3.98
80_60	24000	297760	1.28	N/A	N/A	2.45
100_60	30000	372200	1.27	N/A	N/A	3.49

Table 2. Comparison of mechanical properties from atomistic and coarse grain models.

Model	B		C_{11}		C_{22}		C_{33}		C_{44}		C_{55}		C_{66}	
	MD	CG	MD	CG	MD	CG	MD	CG	MD	CG	MD	CG	MD	CG
20_30	12.04	10.38	13.54	12.19	13.38	12.19	13.53	12.27	2.25	2.72	2.01	2.72	2.24	2.83
15_40	10.73	9.00	12.32	10.95	12.24	10.99	12.27	10.97	2.39	2.92	2.26	2.98	2.31	2.95
30_40	9.79	10.85	11.20	12.80	11.04	12.89	11.19	12.90	2.12	2.93	1.88	3.06	2.10	3.08
40_40	11.99	10.82	13.32	12.67	13.38	12.57	13.22	12.69	1.99	2.78	2.08	2.63	1.84	2.81
80_60	N/A	12.50	N/A	14.72	N/A	14.81	N/A	14.82	N/A	3.33	N/A	3.46	N/A	3.48

From the above we observe the following:

- Densities estimated for both model agrees reasonably well. Same observation is also valid for the stiffness constants.
- The dielectric constant values are comparable to those obtained from atomistic simulation. The average value estimated in both models is ~ 3.0, although the MD model shows larger variations.

This is a significant outcome backing our coarsened model for dielectric properties. This outcome solidifies the foundation of the coarsened model we have developed in this work.

Chain dynamics plays a major role in polymer physics. Although our coarsened model of the piezoelectric polymer could describe polymer bulk properties reasonably well, it was also

important to inspect polymer properties at the chain level to understand the pros and cons of our model with physical explanation.

Table 2. Comparison of polymer chain properties from atomistic and coarse grain models.

	μ_{R_e} (A)		σ_{R_e}		μ_{R_g} (A)		σ_{R_g}	
	MD	CG	MD	CG	MD	CG	MD	CG
10_30	53.18	51.77	24.47	20.17	26.03	23.19	4.13	3.99
20_30	49.29	58.14	22.36	27.23	22.68	31.7	3.93	11.67
15_40	46.28	81.63	15.86	32.6	24.67	43.29	4.38	12.3
30_40	52.15	83.95	22.94	39.83	24.98	41.47	4.46	14.63
40_40	55.39	83.35	18.41	46.29	26.28	40.57	4.33	17.06
80_60	N/A	62.69	N/A	25.08	N/A	30.82	N/A	5.73
100_60	N/A	134.84	N/A	57.78	N/A	60.05	N/A	22.70

Table 3 illustrates the comparison of chain properties of the polymer samples as estimated from MD simulation and coarse-grained model. We find that the chain properties were found to be in excellent agreement for the model polymer considered in building the CG model from atomistic simulation data. The comparison shows also reasonable agreement for the 20_30 polymer case.

4. Dynamic Stress Test of Polymer Models

4.1 Step Stress Test

To test our model's ability to represent polymer's plastic behavior axial tensile stress was applied in z direction of the polyimide and the response was noted. Figure 2 illustrates the instantaneous response of 100_60 polyimide from compressive and tensile stress. In similar lines with its atomistic counterpart, we observe stiffer compressive elastic and yield modulus.

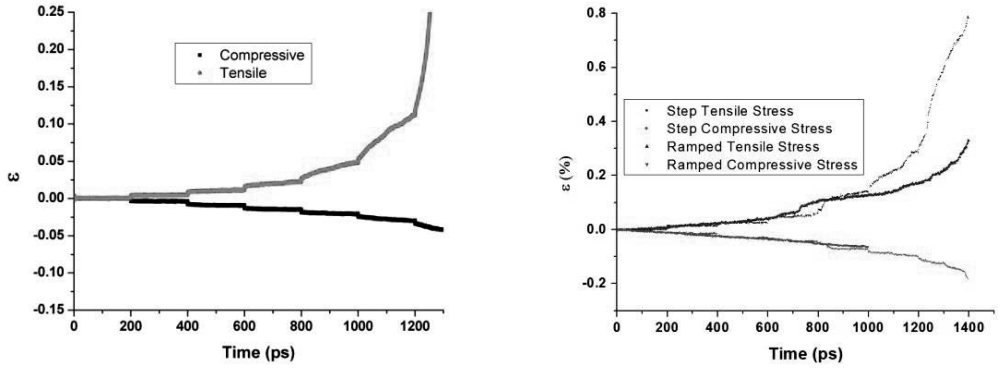

Figure 2. Instantaneous strain response observed for CG (left) and MD (right) model

4.2. Work Hardening

We were also able to reproduce the work hardening effect in the polymer. Figure 3 illustrates the effect of work hardening in a 100_60 polymer sample. We observe identical responses within the elastic region of the polymer sample. Once the sample is out of that elastic response zone the

stretched polymer sample shows more resistance to the applied stress than the initially built equilibrated sample.

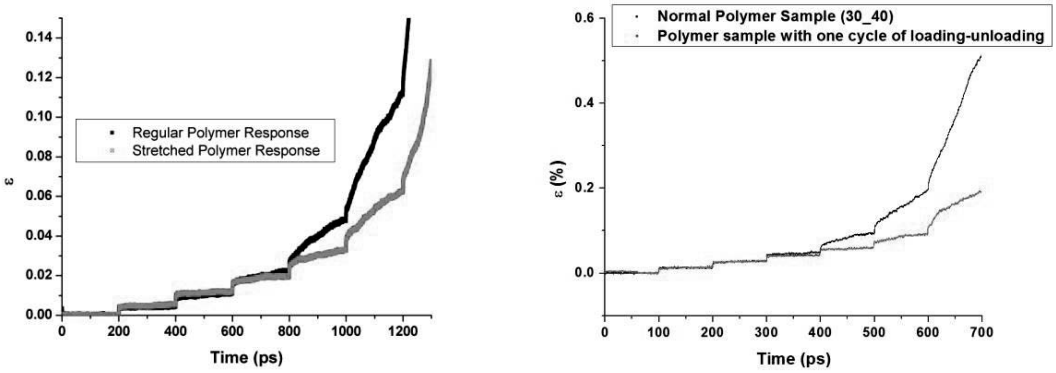

Figure 3: Work hardening observed in CG (left) and MD (right) model of polymer

5. Concluding Remarks

We observe in Figure 4 that the CG model developed shows a 200-300 times gain in terms of CPU time (while maintaining reasonable match in properties as shown in previous sections). The apparent reduction in gain for higher number of processors is due to the higher percentage contribution of communication time between processors as oppose to the calculation of the model itself.

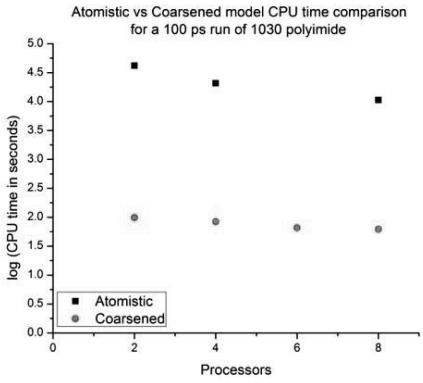

Figure 4: CPU time comparison semi log scale

We have showed that the methodology used in generating the coarse-grained model produced outcomes agreeing reasonably in terms of equilibrium properties, chain properties, mechanical, and dielectric properties as estimated through atomistic simulations. Additionally time dependent properties like the plastic behaviour of polymer and the work hardening were also successfully described by the developed CG approach.

We have obtained two to two-and-half orders of magnitude gain in terms of computational time and an order of magnitude gain in system size through implementation of our coarse grain model.

In conclusion we have developed a coarsened model of a piezoelectric polyimide that could successfully describe the bulk properties including dielectric properties, chain properties and time dependent properties of the system. It can also reproduce the viscoelastic response of the sample under huge stress. It has also succeeded in estimating the thermal, mechanical and dielectric properties barring the effect of rotational degrees of freedom. Incorporation of the same through implementation of rigid body dynamics is expected to better the present model. The substantial gain in terms of CPU time and the opportunity to extend the system sizes is

encouraging. It is thus possible to reliably access domain not accessible to MD by coarsening a system in the way described in this article.

References

1. Baschnagel, J.; Binder, K.; Doruker, P.; Gusev, A. A.; Hahn, O.; Kremer, K.; Mattice, W. L.; Muller-Plathe, F.; Murat, M.; Paul, W.; Santos, S.; Suter, U. W.; Tries, V. In Advances in Polymer Science: Viscoelasticity, Atomistic Models, Statistical Chemistry; Springer-Verlag Berlin: Berlin, 2000, p 41-156.
2. Molinero, V.; Goddard, W. A. J Phys Chem B 2004, 108(4), 1414-1427.
3. Cagin, T.; Wang, G. F.; Martin, R.; Zamanakos, G.; Vaidehi, N.; Mainz, D. T.; Goddard, W. A. Computational and Theoretical Polymer Science 2001, 11(5), 345-356.
4. Zhou, J.; Thorpe, I. F.; Izvekov, S.; Voth, G. A. Biophysical Journal 2007, 92(12), 4289-4303.
5. Tschop, W.; Kremer, K.; Batoulis, J.; Burger, T.; Hahn, O. Acta Polym 1998, 49(2-3), 61-74.
6. Srinivas, G.; Klein, M. L. Molecular Physics 2004, 102(9-10), 883-889.
7. Izvekov, S.; Voth, G. A. J Phys Chem B 2005, 109(7), 2469-2473.
8. Ensing, B.; Nielsen, S. O.; Moore, P. B.; Klein, M. L. Abstr Pap Am Chem Soc 2005, 229, U771-U771.
9. Ayton, G. S.; Voth, G. A. Biophysical Journal 2004, 87(5), 3299-3311.
10. Molinero, V.; Cagin, T.; Goddard, W. A. J Phys Chem A 2004, 108(17), 3699-3712.
11. Kremer, K.; Muller-Plathe, F. Mol Simul 2002, 28(8-9), 729-750.
12. Tozzini, V. Curr Opin Struct Biol 2005, 15(2), 144-150.
13. Santangelo, G.; Di Matteo, A.; Muller-Plathe, F.; Milano, G. J Phys Chem B 2007, 111(11), 2765-2773.
14. Milano, G.; Muller-Plathe, F. J Phys Chem B 2005, 109(39), 18609-18619.
15. Izvekov, S.; Violi, A.; Voth, G. A. J Phys Chem B 2005, 109(36), 17019-17024.
16. Liu, P.; Izvekov, S.; Voth, G. A. Biophysical Journal 2007, 566A-566A.
17. Groot, R. D.; Warren, P. B. J Chem Phys 1997, 107(11), 4423-4435.
18. Ortiz, V.; Nielsen, S. O.; Discher, D. E.; Klein, M. L.; Lipowsky, R.; Shillcock, J. J Phys Chem B 2005, 109(37), 17708-17714.
19. Reith, D.; Putz, M.; Muller-Plathe, F. J Comput Chem 2003, 24(13), 1624-1636.
20. Hone, T. D.; Izvekov, S.; Voth, G. A. J Chem Phys 2005, 122(5), 7.
21. Molinero, V.; Cagin, T.; Goddard, W. A. Chem Phys Lett 2003, 377(3-4), 469-474.
22. Ensing, B.; Nielsen, S. O.; Moore, P. B.; Klein, M. L. Abstr Pap Am Chem Soc 2004, 228, U221-U221.
23. Srinivas, G.; Lopez, C. F.; Klein, M. L. Abstr Pap Am Chem Soc 2004, 228, U221-U221.
24. Saiz, L.; Klein, M. L. Accounts of Chemical Research 2002, 35(6), 482-489.
25. Srinivas, G.; Discher, D. E.; Klein, M. L. Nat Mater 2004, 3(9), 638-644.
26. Abrams, C. F.; Delle Site, L.; Kremer, K. Multiscale Computer Simulations for Polymeric Materials in Bulk and Near Surfaces; Physics and Astronomy, 2002.
27. Maiti, P. K.; Li, Y.; Çağın, T.; Goddard, W. A. Macromolecules 2007, Submitted.
28. Wang, Y. T.; Izvekov, S.; Yan, T. Y.; Voth, G. A. J Phys Chem B 2006, 110(8), 3564-3575.
29. Izvekov, S.; Voth, G. A. J Chem Phys 2005, 123(13), 13.

Construction of Nanostructures and Materials through Peptide or Charged Block Copolymer Self-assembly

Darrin Pochan

University of Delaware, Newark, DE 19716
(E-mail: Pochan@udel.edu)

ABSTRACT

Bionanotechnology, the emerging field of using biomolecular and biotechnological tools for nanostructure or nanotechnology development, provides exceptional opportunity in the design of new materials. Self-assembly of molecules is an attractive materials construction strategy due to its simplicity in application. By considering peptidic or charged synthetic polymer molecules in the bottom-up materials self-assembly design process, one can take advantage of inherently biomolecular attributes; intramolecular folding events, secondary structure, and electrostatic interactions; in addition to more traditional self-assembling molecular attributes such as amphiphilicty, to define hierarchical material structure and consequent properties. First, design strategies for materials self-assembly based on small (less than 24 amino acids) beta-hairpin peptides will be discussed. Self-assembly of the peptides is predicated on an intramolecular folding event caused by desired solution properties. Importantly, kinetics of self-assembly can be tuned in order to control gelation time allowing for cell encapsulation. The final gel behaves as a shear thinning, but immediately rehealing, solid that is potentially useful for cell injection therapies. Second, synthetic block copolymers with charged corona blocks can be assembled in dilute solution containing multivalent organic counterions to produce novel micelle structures such as toroids. Micelle structure can be tuned between toroids, cylinders, and disks simply by using different concentrations or molecular volumes of organic counterion the kinetic pathway of assembly. The kinetics of block copolymer assembly can be specifically controlled to form hierarchically structured morphologies not possible through traditional block copolymer self-assembly.

New Proposed Mechanism for Actin-Polymerization-Driven Motility

Andrea Liu, Kun-Chun Lee

**Department of Physics and Astronomy, University of Pennsylvania,
Philadelphia, PA 19104, USA
(E-mails: ajliu@physics.upenn.edu, kunchun@sas.upenn.edu)**

ABSTRACT

When a cells crawls, its shape re-organizes via polymerization and depolymerization of a network of actin filaments. The growing ends of the filaments are localized near the outside of the cell, and their polymerization, regulated by a host of proteins, pushes the cell membrane forwards in a biological model known as the dendritic nucleation model. The same dendritic nucleation mechanism comes into play when the bacterial pathogen Listeria monocytogenes infects a cell. The bacterium hijacks the host cell's actin machinery to create an actin network (the actin comet tail) that propels the bacterium through cells and into neighboring cells. I will discuss recent results from Brownian dynamics simulations that suggest a new picture for the physical mechanism underlying this form of motility. In this picture, the dendritic nucleation mechanism recruits actin near the back end of the bacterium. If the surface of the bacterium repels actin, however, it will move forwards to lower the concentration near the surface. I will also present estimates of the effect of flow on the motion; when flow is included, motion results from the phenomenon known as self-diffusiophoresis

Computational Modeling of Complex Fluids – Scaling Properties of Flexible and Semiflexible Polymer Chains

Julian Schneider[1], Martin O. Steinhauser[2]

[1]Fraunhofer Institute for Mechanics of Materials (IWM), Wöhlerstrasse 11, D-79108 Freiburg, Germany (E-mail: Julian.Schneider@iwm.fraunhofer.de)
[2]Fraunhofer Ernst-Mach Institute for High-Speed Dynamics (EMI), Eckerstrasse 4, D-79104 Freiburg, Germany (E-mail: Martin.Steinhauser@emi.fraunhofer.de)

ABSTRACT

The conformational and scaling properties of flexible long linear and branched polymer chains are investigated using combined Monte Carlo and Molecular Dynamics (MD) simulations. Computational methods for the efficient simulation of such polymer systems in solution and in the melt are shortly discussed and numerical examples are provided [1-3]. Chain lengths that comprise several orders of magnitude are used to reduce errors of finite size scaling. The effects of solvent quality, from good solvent and θ-conditions to the collapsed state, are included in the investigations of the scaling behavior of the polymer chains. Results of chain properties in the extrapolated limit of infinite chain length are provided and their universal properties which span over many length scales within their universality class are discussed. We also present MD simulations of semiflexible polymer systems (single chains and in the melt) and focus here on the crossover between different scaling regimes and on the change of the respective scaling exponent. The transition from flexible to semiflexible chain behavior is investigated by systematically increasing the persistence length which is controlled in the simulation by a single parameter. Our simulation results of semiflexible chains are analyzed by performing a Rouse normal mode analysis. As a result we observe a crossover in the scaling behavior of the mean square normal mode amplitudes and the corresponding relaxation times with increasing mode number p from a well-known Rouse-like p^{-2}-scaling to a distinct p^{-4}-scaling. This crossover scaling behavior has been reported here for the first time in a simulation study. A pronounced shift of the crossover region is observed upon increasing the stiffness. Similar results are found for the monomer dynamics as well as for the structure function.

[1] M.O. Steinhauser, "Computational Multiscale Modeling of Fluids and Solids – Theory and Applications", Springer, Berlin, Heidelberg, New York (2008).
[2] M. O. Steinhauser, "Computational Methods in Polymer Physics", in: Recent Res. Devel. Physics, pp. 59-97, Transworld Research Network, Trivandrum, India (2006).
[3] M.O. Steinhauser, "A Molecular Dynamics Study on Universal Properties of Polymer Chains in Different Solvent Qualitites. Part I. A Review of Linear Chain Properties", J. Chem. Phys., **122**, 094901 (2005).

Financial support by the Fraunhofer-Gesellschaft e.V. Germany with grant No. 100129 (Hochfeste Kunststoffe) is gratefully acknowledged.

Atomistic Modelling of Biomolecular Adhesion on Materials Surfaces

Lucio Colombi Ciacchi[1,2], Daniel J. Cole[3], Mohammad Koleini[1,2], Peter Gumbsch[1,2]

[1]Institute for Reliability of Components and Systems, University of Karlsruhe, Germany, (E-mail: lucio@izbs.uni-karlsruhe.de)
[2]Fraunhofer Institute for Mechanics of Materials, Freiburg, Germany;
[3]Theory of Condensed Matter Group, Cavendish Laboratory, University of Cambridge, UK.

ABSTRACT

The adsorption of biomolecules on solid materials surfaces is a phenomenon of large scientific and technological relevance in a vast number of biomedical and biotechnological applications. A thorough understanding of the adsorption processes at the atomic scale is very desirable in order to improve the performances of materials in contact with biological soft tissues, but is hindered by the intrinsic complexity of the phenomena involved. These comprise chemical oxidation reactions of the surfaces in contact with physiological fluids, adsorption of metal ions on the oxidised surfaces, physical and chemical interactions with the amino acid residues of the adsorbing proteins, as well as rearrangement and partial denaturation of the protein structure as a consequence of strong protein/surface interactions. Atomistic modelling of biomolecular adsorption on materials surfaces therefore spans over different time and size scales, and require treatments both at the quantum and at the classical levels of precision. We will present results of molecular dynamics investigations of both the formation of native oxide structures on various metallic and semiconducting materials and of the adsorption of protein fragments on the obtained surface models. Our atomistic simulations are performed with a hierarchical approach in which chemical and structural information obtained on the quantum scale [1] is implemented into carefully tuned classical force-fields [2]. Large-scale simulations of protein adsorption reveal non-trivial adhesion mechanisms, which are partially driven by the structuring of water molecules at the solid/liquid interface [3]. Moreover, the mechanical properties of the biomolecules are observed to have a direct influence on the calculated adhesion forces. This information can be of great help for the rational design of adhesives for medical applications on a biomolecular basis.

[1] L. Colombi Ciacchi, M. C. Payne, "First principles molecular dynamics study of native oxide growth on Si(001)", Physical Review Letters **96**, 196101 (2005).
[2] D. J. Cole, G. Csányi, M. C. Payne, S. M. Spearing, L. Colombi Ciacchi, "Development of a classical force field for the oxidised Si surface: Application to hydrophilic wafer bonding", *Journal of Chemical Physics* **127**, 204704 (2007).
[3] D. J. Cole, M. C. Payne, L. Colombi Ciacchi, "Biomolecular adsorption at a silicon-water interface driven by water-structure effects", submitted (2008).

The authors acknowledge support by the Deutschen Forschungsgemeinschaft within the Emmy Noether Programme

Simulating Folding and Interaction of Proteins

Ulrich H.E. Hansmann

Dept. of Physics, Michigan technological University, 1400, Townsend Dr., Houghton, MI 49931, USA
(E-mail: hansmann@mtu.edu)

ABSTRACT

Proteins are nanomachines that perform a large number of diverse functions in cells. Despite decades of research we still do not understand in complete detail the mechanism by which a protein folds into its biologically active form. Computational tools that allow one to evaluate the sequence-structure relationship and the folding process would therefore lead to a deeper insight into the molecular machinery of cells. Unfortunately, computer simulations are extremely difficult for detailed protein models. This is because the energy landscape of all-atom protein models is characterized by a multitude of local minima separated by high energy barriers. Only over the last few years have been algorithms developed that allow one to overcome this multiple-minima problem. I will discuss some of these techniques and their application to studies of folding, mis-folding and interaction of proteins.

Umbrella Sampling For Non-Equilibrium Processes

Aryeh Warmflash[1], Alex Dickson[1], Prabhakar Bhimalapuram[1], Aaron R. Dinner[1]

[1]James Franck Institute, The University of Chicago, Gordon Center for Integrative Science, 929 E 57th St, Chicago, IL 60637 (E-mail: dinner@uhicago.edu)

ABSTRACT

Many systems of significant fundamental and applied interest are microscopically irreversible. For theoretical studies of such systems, the steady-state distribution is of central importance because it enables calculation of static averages of observables for comparison to experimental measurements. For systems at equilibrium, low probability states can be explored efficiently in simulations with umbrella sampling methods, in which biasing potentials that are functions of one or more order parameters are used to enhance sampling of selected regions of phase space. What complicates extending umbrella sampling to simulations of non-equilibrium processes is that, by definition, they do not obey detailed balance (microscopic reversibility). As such, one must account for the fact that the steady-state probability of observing particular values of the order parameters can be determined by a balance of flows in phase space through different possible transitions. In this talk, I will describe an algorithm for enforcing equal sampling of different regions of phase space in an ergodic system arbitrarily far from equilibrium, which enables its steady-state probability distribution to be determined with high accuracy [1]. Applications and extensions of the method will be discussed.

[1] A. Warmflash, P. Bhimalapuram, and A. R. Dinner, "Umbrella sampling for nonequilibrium processes", Journal of Chemical Physics, **127,** 154112 (2007).

This work is supported by the National Science Foundation and Natural Sciences and Engineering and Research Council.

Multi-Scale Sampling Design for Biomolecular Simulations

Wei Yang

Florida State University, Tallahassee, FL, USA
(E-mail: wyang@scs.fsu.edu)

ABSTRACT

In this talk, a general strategy for the sampling design will be presented. Specifically, the design for the employment of generalized ensemble method in free energy simulations will be discussed.

Forced Dynamics and Stability of RNA Nanostructures

Maxim Paliy[1], Roderick Melnik[1], Bruce Shapiro[2]

[1] M²NeT Lab, Wilfrid Laurier University, Waterloo, ON, Canada, N2L 3C5, http://www.m2netlab.wlu.ca; mpaliy@wlu.ca; rmelnik@wlu.ca
[2] Center for Cancer Research Nanobiology Program, National Cancer Institute, Frederick, MD 21702, bshapiro@ncifcrf.gov

ABSTRACT

We study the mechanical and thermodynamic properties of a hexagonal RNA nanoring structure [Y.G.Yingling, B.A.Shapiro, NanoLett. 7 (2007)] focusing on the following issues: (i) stability of the nanoring versus temperature; (ii) effect of the environment (solvent, counter-ions); (iii) conformations and dynamics under external force. Evaporation of the ions from the ring upon decrease of temperature has been observed, demonstrating a surprising feature - the uptake of ions by the ring grows with the temperature. Several key properties of the nanoring, such as elastic coefficient and damping coefficient in water, have been determined. A measure of the tensile elasticity of the ring against its uniform 2D in-plane compression yields the value of K_{eff} < 0.013 GPa, which is much lower than typical values found for soft matter other than RNA.

1. Introduction

Recently, RNA has been proposed as a promising alternative to DNA and proteins for the design of artificial self-assembled materials at a nanoscale [1,2]. RNA (as compared to DNA) offers (i) much greater variety of interactions, as well as (ii) enhanced conformational flexibility, that is not only already used by Nature via the ubiquitous catalytic function of RNA, but it also makes RNA an interesting material for use in the man-made molecular machines. That is why the study of the "functional behavior" of RNA nanostructures (externally controlled conformational changes, e.g. elbow-like motions in a "kink-turn motif" [3, p.320], or isomerisation of the "kissing-loop motif" [4]) is important. To date, only limited data about thermal stability/dynamics of such nanostructures are available [1-3] from experiments and simulations, while the "functional" aspect has been largely overlooked, and a complete picture of RNA nanostructures behavior (esp. under an external forcing) is required.

In this paper we present all-atom classical Molecular Dynamics (MD) results on the stability and dynamics of a simple RNA nanostructure (~13 nm in size) – hexagon-shaped RNA ring [2], composed of 6 "RNAIi/RNAIIi complexes", joined by "kissing loop" motifs (Fig. 1, left). Firstly, the behaviour of the nanoring upon the temperature change is determined. Secondly, the response of the nanostructure to the combined action of the temperature and applied external forces is studied in some detail. One of the emphases of this work is on the effect of the counter-ions and solvent [5]. Finally, dictated by the slowness of MD simulations, the development a coarse-grained model [6], suitable for the description of RNA nanostructures, is in progress.

2. Model and Methods

We use NAMD/VMD packages [7] for all-atom MD simulation/visualisation of the RNA nanoring with the CHARMM27 force field. For the purposes of this study, the RNA nanoring is solvated in 88664 TIP3P water molecules (box ~180x180x90 Angstroms), together with a varied number of ions - 330 Na^+ or 165 Mg^{2+} ions are added to neutralize 330 phosphates, and some extra Na^+, Mg^{2+}, and Cl^- ions are added in order to represent a range of solutions from "physiological" to "sea water". The system is simulated at constant temperature T (via Langevin method) and pressure P=1 atm (via Nose-Hoover Langevin piston) with periodic boundary conditions in all 3D. The time step is 2 fs and non-bonded interactions cutoff is 12 Angstroms.

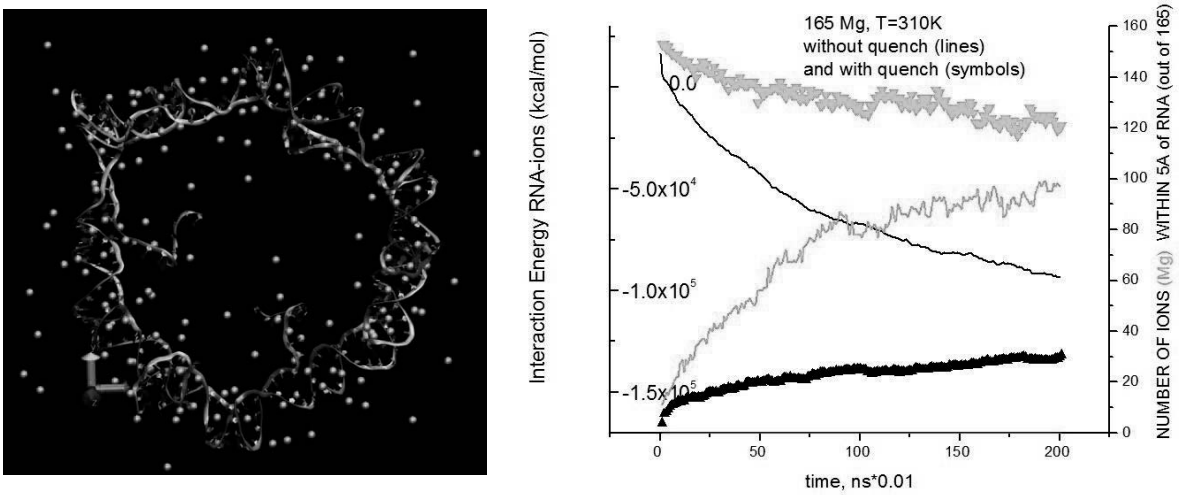

Figure 1. Left: *RNA nanoring solvated in a water box (not shown) together with the Mg^{2+} counter-ions (green spheres).* Right: *The energy of interaction "RNA - ions" (black) and the number of Mg ions found within 5 Angstroms of RNA (green) versus time at 310K. The "quenched" dependencies (as explained in Sec. 3) are shown with the symbols, while those for the runs that started from an initial non-solvated configuration are shown with solid lines.*

3. The effect of the temperature and the ions on the nanoring

We study the thermal stability of the RNA nanoring in the range of temperatures (310K to 510K). Our results demonstrate the intricate role of the ions in a series of "quenched" runs (i.e. when the ring, equilibrated at higher temperature of 510K, is subsequently subjected to a lower temperature of 310K). Surprisingly, the quench leads to the evaporation of the ions from the ring into the solution, as illustrated in Fig.1, right (such evaporation occurs for both Mg and Na ions). From Fig.1 and similar data for Na, one can estimate that at higher T=510K the ring takes up more ions (e.g. 0.8 Na per phosphate or 0.88 Mg per 2 phosphates), as compared to T=310K (0.6 Na or 0.66 Mg, respectively). Since the counter-ions are known to be an important factor in stabilization of the native folds of the biopolymers, *the observed higher uptake of ions by the RNA ring at higher temperature may mean that the RNA ring demonstrates, in a sense, a mechanism of "self-stabilization" upon increase of temperature.*

However, the origin of this phenomenon remains rather puzzling to us. It contradicts (i) simple chemical equilibrium ideas (van't'Hoff equation); and (ii) Manning condensation theory describing the adsorption of ions onto charged polymers in the solutions (the latter is not applicable directly, because of circular instead of linear geometry, and the ring thickness comparable to the Debye length). One may speculate that the thermal contraction of the ring leads to the evaporation of the ions (in the range 510-310K the ring contracts about 5%, or 10%-15% in terms of volume, roughly the same as pure water); however, the percentage of ions evaporated is higher (17% - 27%). Other hypotheses should be explored, e.g. some (yet to be identified) structural change in the RNA ring with temperature (the changes of the hydration state of the solutes, in particular biological ones [8], are known to modify also their solubility).

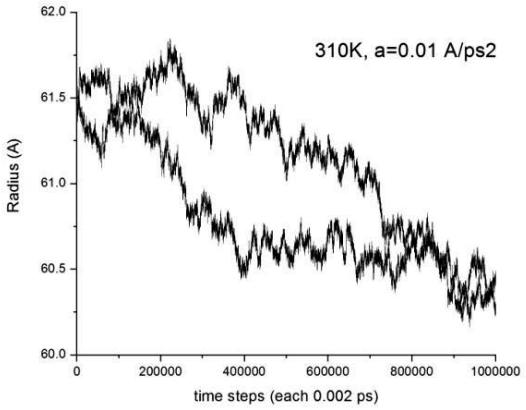

Figure 2. Left: *Gyration radius R(t) of the RNA ring subjected to a small constant compressive force a = 0.01 A/ps^2. Two independent runs are shown.* Right: *Snapshot of the RNA ring subjected to extreme compression by quasi-linearly increasing force, at a = 1.7 A/ps^2.*

4. Forced dynamics of the nanoring

"Steered MD" functionally of NAMD has been used to apply uniform compressive/expansive force, that is directed towards the centre of mass of the RNA ring, to 2130 atoms of its nucleic acid backbone (this setup, dictated by geometry, allows one to estimate average properties of the ring). Since the strength of the ring is mainly determined by hydrogen bonding, the total force applied to the ring should not exceed ~100 pN, i.e. ~0.05 pN per atom (~0.02 A/ps^2 in the units of acceleration used). However, the response of the ring to such weak forcing is expected to be extremely slow, ~μs, which cannot be achieved in our MD simulations. In attempts to circumvent this difficulty, we studied the dynamics of the ring within a range of forces, 10^{-2} - 1 A/ps^2. The evolution of the gyration radius of the ring *R(t)* has been monitored.

Under the application of an intermediate dc force, a=0.1 A/ps^2, the *R(t)* dependencies are linear, i.e. the ring shows a behaviour compatible with a drift of an overdamped non-interacting particle subjected to a constant force. Namely, *R(t)* can be found from $m\eta_{eff}\dot{R} = ma,$ where η_{eff} is an effective damping for RNA fragments in water, that can be determined from the slope of a *R(t)* dependence, $\eta_{eff} \approx 56\,\mathrm{ps}^{-1}$ at T=310K, and $\eta_{eff} \approx 29\,\mathrm{ps}^{-1}$ at T=510K. One can further estimate

the activation energy from the Arrhenius formula $\eta_{eff} = \eta_0 \exp(E_a / k_B T)$, as $E_a \approx 450K$. We tried to elucidate the ring elasticity in this regime, by collecting the energies E of the configurations obtained during the "compression drift", and plotting them against R, but the resulting $E(R)$ turned out to be non-parabolic, and therefore an elastic coefficient could not be determined, probably because the used configurations are not at equilibrium.

A series of longer (*2* ns) runs have been carried out at a small force, $a=0.01\ A/ps^2$ (~ two times less the one needed to break hydrogen bonds in our setup). Fig. 2, left, shows that even if the equilibrium is not yet achieved after *2 ns*, the system spends a long time (> *200 ps*) in the plateaux of $R(t)$ dependence, before jumping to a next plateau, and the hypothesis of a free forced drift no longer applies. From the data of Fig. 2, left, one can give an *upper* estimate for the elasticity of the RNA ring in the following way. In the plane of the ring, the 2D equation analogous to the one for the bulk modulus in 3D, reads: $dP = -K_{2D} dS / S$, where dS is the change in ring's surface upon the change in "2D pressure", $dP = aM / (2\pi R)$, where M is the total mass of the nucleic acid backbone. Since from Fig. 2, left, one can judge that $dR_g \geq 1.3A$, and $dS / S = 2dR / R$, one obtains an estimate, $K_{2D} \leq 0.04$ N/m. In order to compare it with a 3D measure of elasticity, one can divide K_{2D} by the (approximately constant) thickness of the ring in a normal direction, *~30 A*, to obtain $K_{eff} \leq 0.013\,GP$a. This is a much lower value compared to those for soft matter other than RNA (typical values for DNA Young modulus are *~0.1 GPa*).

Finally, under the action of a very strong compressive force, the ring starts to fold into a triangular shape (Fig. 3, right), where three of the six "kissing loops" form the angles and three remaining ones belong to the sides of the triangle.

Acknowledgements

M.P. and R.M. are grateful to the NSERC and the CRC Program for the support and to Sarah Woodson for helpful comments. This work was made possible by the facilities of the Shared Hierarchical Academic Research Computing Network (SHARCNET: www.sharcnet.ca), and was supported in-part by the intramural research program of the NIH, National Cancer Institute, Center for Cancer Research.

References

[1] Luc Jaeger and Arkadiusz Chworos, Curr. Opinion Struct. Biol., 16 (4), 531-543, 2006.
[2] Y. G. Yingling, B. A. Shapiro, Nano Letters, 7, 2328-2334, 2007.
[3] Computational studies of RNA and DNA. Series: Challenges and Advances in Computational Chemistry and Physics , Vol. 2, Šponer, Jirí; Lankaš, Filip (Eds.) 2006, XI, 638 p.
[4] Xianglan Li, Satoru Horiya, and Kazuo Harada, J. Am. Chem. Soc., 128, 4035-4040, 2006.
[5] M.Paliy, R. Melnik, B.Shapiro, to be submitted (2008).
[6] V.Tozzini, Curr. Opinion Struct. Biol. 15,144-150, 2006.
[7] W. Humphrey, A. Dalke and K. Schulten, J. Mol. Graphics 4 (1996), pp. 33-38; James C. Phillips et al. , Journal of Comp. Chemistry, 26:1781-1802, 2005.
[8] Peter. J. Mikulesky and Andrew L. Feig, Biopolymers, 82 (1), 38 (2006).

Dynamics of Polymers Adsorbed on Lipid Bilayers

S. P. Adiga[1], T. G. Desai [2]

[1]Materials Science Division, Argonne National Laboratory, Argonne, IL 60439
[2]Material Sciences Department, Idaho National Laboratory, Idaho Falls, ID 83415
(E-mails: spadiga@anl.gov, Tapan.Desai@inl.gov)

ABSTRACT

The problem of translational diffusion of adsorbed chain molecules on phospholipid bilayers is not only of fundamental interest in biology but also in applied areas such as drug delivery and smart nanostructures. Experimental investigation of diffusion of DNA molecules adsorbed (dilute coverage) on supported lipid bilayers has showed that the center of mass diffusion coefficient scales with the degree of polymerization as $D \sim N^{-1}$ [1]. Recently, simulations of a single adsorbed polymer chain at a solid-liquid interface have revealed that $D \sim N^{-x}$, with $x = 3/4$ and 1 for smooth and corrugated surfaces, respectively [2]. These simulations substantiate that the diffusion of polymer adsorbed on lipid bilayer is similar to the corrugated surface case where friction of the adsorbed molecule dominates and hydrodynamic coupling between the monomers becomes less important. Here, coarse grained molecular dynamics simulations are performed to investigate the dynamics of polymer chains adsorbed on lipid bilayers. In particular, we will discuss the dynamics of polymer chains at bilayer-water interface with respect to scaling of diffusion coefficient, radius of gyration and relaxation time with degree of polymerization. We will also discuss the effect of polymer adsorption on diffusion of lipid molecules and investigate the phenomenon of slaved diffusion as reported by recent experiments [3].

[1] B. Maier and J. O. Radler, *Phys. Rev. Lett.* **82**,1911 (1999).
[2] T. G. Desai, P. Keblinski, S. K. Kumar and S. Granick, *Phys. Rev. Lett.* **98**, 218301 (2007).
[3] L. Zhang and S. Granick, Proc. Nat. Acad. Sci. 102, 1918 (2005).

Prediction of Protein Functional States by Multi-Resolution Protein Modeling

Cecilia Clementi

Department of Chemistry, Rice University, Houston, Texas 77005
(E-mail: cecilia@rice.edu)

ABSTRACT

The detailed characterization of the overall free energy landscape associated with the folding process of a protein is the ultimate goal in protein folding studies. Modern experimental techniques provide accurate thermodynamic and kinetic measurements on restricted regions of a protein landscape. Although simplified protein models can access larger regions of the landscape, they are oftentimes built on assumptions and approximations that affect the accuracy of the results. We present new methodologies that allows to combine the complementary strengths of theory and experiment for a more complete characterization of a protein folding landscape at multiple resolutions. Recent results on the characterization of the folding landscape of Photoactive Yellow Protein (PYP) will be discussed. PYP is responsible for the bacteria Halorhodospira Halophila's ability to respond to the presence of blue light. It is believed that the detected light is absorbed by a chromophore covalently attached to the protein, and that a resultant photo-isomerization initiates a transformation of the protein to its signaling state. The time scale of the transformation, makes the signaling conformation difficult to crystallize and simulate. The application of our multi-resolution techniques has recently produced a promising candidate for the signaling state.

Runniness and Randomness of Confined Fluids

Thomas Truskett

University of Texas at Austin, Austin, TX 78712, USA
(E-mail: truskett@che.utexas.edu)

ABSTRACT

Fluids trapped in small spaces feature prominently in science and technology, and understanding their properties is critical to progress in fields that range from cell biology to the engineering of nanoscale devices. Interestingly, such "confined fluids" behave differently than bulk samples. Properties strongly affected by confinement include (i) how the particles pack together, (ii) how their thermodynamic state changes under heating or squeezing, and (iii) their tendency to rapidly mix or flow. The first two have been reasonably well understood for some time, but a general rule for even qualitatively predicting the third has proven elusive. In this talk, we highlight how recent theory and molecular simulation have discovered links between the entropy ("randomness") and the dynamics ("runniness") of confined fluids. These links provide new physical insights and allow one to forecast how nanoscale confinement will modify the behavior of bulk materials.

Engineering structure and function with theoretical protein design

Jeffery Saven

University of Pennsylvania, Philadelphia, PA 19104, USA
(E-mail: saven@sas.upenn.edu)

ABSTRACT

Protein design opens new ways to probe the determinants of folding, to facilitate the study of proteins, and to arrive at novel molecules, materials and nanostructures. Recent theoretical methods for identifying the properties of amino acid sequences consistent with a desired structure and function will be discussed. Such methods address the structural complexity of proteins and their many possible amino acid sequences. Computationally designed protein-based systems will be presented that have been experimentally realized, including novel proteins tailored to accommodate nonbiological cofactors

Multiscale modeling of non-linear optical materials for all-optical switching applications

Sergio Tafur[1], Kyrill Suponitsky[2], Talgat Inerbaev[2], Artem Masunov[2]

[1]Department of Physics and Nanoscience Technology Center, University of Central Florida (E-mail: tafur@physics.ucf.edu)
[2]Nanoscience Technology Center, University of Central Florida
(E-mails: kirshik@yahoo.com, inerbaev@yahoo.com, amasunov@mail.ucf.edu)

ABSTRACT

Telecommunication and information technology industries currently experience a steady increase of bandwidth demand. Information transmission and processing systems are already taking advantage of photons as information carriers, due to their much higher speed and density of components, as well as lower power requirements and heat generation. Modern fiber optic systems, however, rely on low-speed (no more then 40 Gbit/s) electronic components for switching, routing and storing information. Higher rates require new concepts in optical switching technology. Different design schemes had been proposed for the optical switching elements. Many of them require the use of nonlinear optical (NLO) materials, which change the refractive index or transparency under the influence of the control beam. The organic materials (both polymer and small molecule based), containing donor/acceptor (D/A) substituted π-conjugated systems possess extremely fast nonlinear optical response time, purely electronic in origin and become promising candidates for optoelectronic applications. Optimization of NLO properties, such as nonlinear refractive index or hyperpolarizability, is of high technological interest. We apply a multi-scale simulation scheme to design NLO materials from oligomer to polymer chain to 3D-crystal. At the monomer scale the electronic structure is described with hybrid Density Functional Theory (DFT), while NLO properties are predicted with Sum over States (SOS) formalism. To calculate the permanent dipole moments of the excited states and transition dipole moments between the excited states, we use a posteriori Tamm Dancoff approximation (ATDA), recently introduced, implemented, and validated against highly correlated Coupled-Cluster methods [1]. At the mesoscale the excitation energies and transition dipole moments of the oligomer are extrapolated to extended polymer chains and used to predict NLO response of 1D-periodical system. Aggregation of the polymer chains and their 3D-packing structure result in the appearance of new excited states, in addition to intra-chain excitations. The arrangements of the polymer chains in the material are predicted by the molecular dynamics simulations. We apply the described multi-scale approach to the 6 crystals with large second and third-order susceptibilities (MNA, COANP, PNP, MNBA, DANS, and DANPH) [2]. Predictions of nonlinear optical properties and crystal structure for these crystals are compared to the experimental results.

[1] I. A. Mikhailov, S. Tafur, and A. E. Masunov, Double excitations and state-to-state transition dipoles in π-π* excited singlet states of linear polyenes: Time-dependent density-functional theory versus multiconfigurational methods. Phys. Rev. A 77, 012510 (2008)
[2] C. Bosshard, G. Knopfle, P. Pretre, S. Follonier, C. Serbutoviez, P. Gunter, Molecular crystals and polymers for nonlinear optics. Optical Engineering. 34(7), 1951-1960 (1995)

Hierarchical Modeling of the Mechanical Properties of Lobster Cuticle from Nano- Up to Macroscale: The Influence of the Mineral Content and the Microstructure

Svetoslav Nikolov[1], Christoph Sachs[1], Helge Fabritius[1], Dierk Raabe[1], Michal Petrov[2], Martin Friák[2], Jörg Neugebauer[2], Liverios Limperakis[2], Duancheng Ma[1]

Max-Planck-Institut für Eisenforschung, [1]Department of Microstructure Physics and Metal Forming; [2]Department of Computational Materials Design
Max-Planck-Str. 1, 40237 Düsseldorf, Germany
(E-mails: s.nikolov@mpie.de, c.sachs@mpie.de, h.fabritius@mpie.de, d.raabe@mpie.de, m.petrov@mpie.de, m.friak@mpie.de, j.neugebauer@mpie.de, l.limperakis@mpie.de, d.ma@mpie.de)

ABSTRACT

We propose a hierarchical model for the prediction of the elastic properties of a mineralized lobster cuticle using i) *ab initio* calculations for the properties of chitin and ii) hierarchical homogenization performed in a bottom-up order for all hierarchy levels. The lobster cuticle is a mineralized organic tissue reinforced with chitin-protein fibers. We compare the model predictions to experimental data for the Young moduli of wet lobster endocuticle. It is found that the dominant factors determining the cuticle stiffness are i) the mineral content, ii) the microstructure of the mineral-protein matrix and iii) the in-plane area fraction of the pore canals. Our results suggest that the mineral-protein matrix most likely consists of amorphous calcium carbonate spheres with varying diameters embedded in proteins and arranged in a microstructure known as symmetric cell material. Most of the scattering in the experimentally measured Young moduli can be explained by the observed biological variation in the area fraction of the pore canals.

1. Introduction

Structural biomaterials have hierarchically organized microstructure and are known to possess exceptional mechanical properties (e.g., in terms of stiffness-to-density ratio and fracture toughness), the origin of which has become subject of intensive research in the recent years. The overall properties of these materials depend on the specific microstructure and properties at all levels of hierarchy. Here we focus on the multiscale modeling of the structure/properties relations and the design principles embedded in the mineralized cuticle of the crustacean *Homarus americanus*. The structure/properties relations in mineralized cuticles have received relatively little attention in the literature, despite the fact that they are the main hard tissue in arthropods, which account for about 80% of all animals living on Earth. Recently, extensive experimental work provided a more detailed knowledge about the structure and the mechanical

properties at the micro- and the nanoscale of the cuticle of the lobster *Homarus americanus* [1], the hierarcucal microstructure of which is shown in Fig. 1.

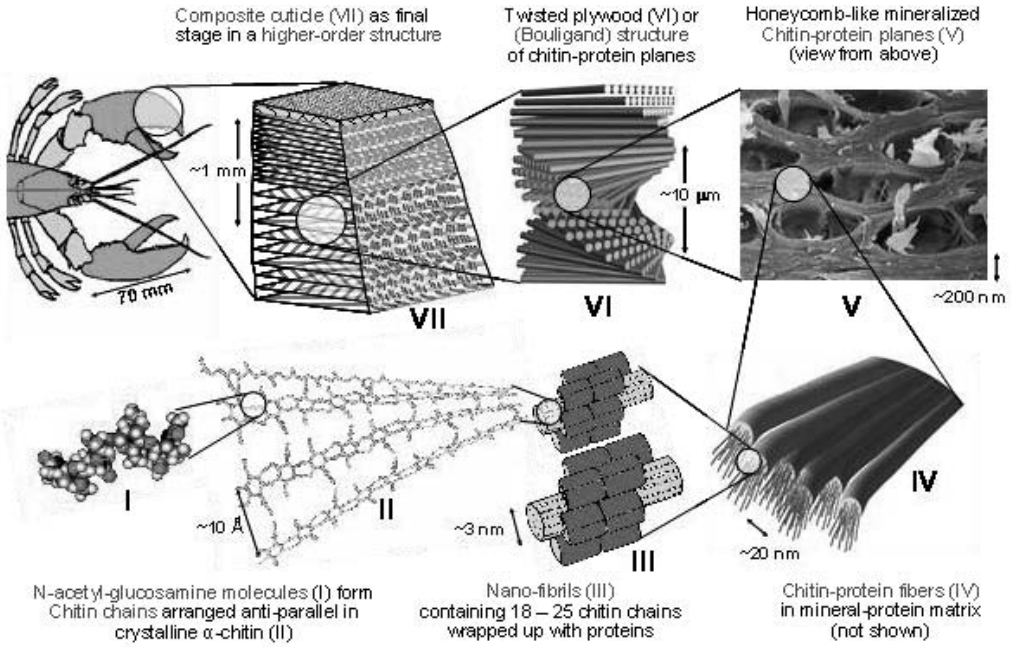

Figure 1. Hierarchical microstructure of lobster cuticle. From bottom-left counter-clockwise: N-acetyl-glucosamine molecules (**I**); anti-parallel chains of α-chitin (**II**); nanofibrils of crystallized chitin chains wrapped with proteins (**III**); chitin-protein fibers (**IV**) embedded in mineral-protein matrix; in-plane cross section of the cuticle with elliptic canal openings (**V**); twisted plywood (Bouligand) structure (**VI**); 3-layered cuticle (**VII**). Bottom layer: endocuticle; middle layer: exocuticle; outer thin waxy layer.

We propose a multiscale constitutive model for the effective elastic properties of a mineralized lobster cuticle. The elastic properties are found at each level of hierarchy in a bottom-up order. For a given level, we define a Representative Volume Element of the heterogeneous material and find its homogenized properties. These properties are then injected in the modeling of the microstructure at the next higher level. The procedure is repeated to cover all observed microstructures at all length scales from 10^{-9} to 10^{-3} m. Recently, a similar approach has been applied to evaluate the effective stiffness tensor of bone at submicron length scales [2]. In addition to the mean-field homogenization methods, we use *ab initio* calculations to determine the elastic properties of crystalline α-chitin, a structural biopolymer that plays a crucial role in the exoskeleton tissues of arthropods. The model predictions for the effective Young moduli are compared to experimental data from tension and compression tests performed on hydrated lobster endocuticle.

2. Hierarchical Modeling

The 3D elastic constants of crystallized α-chitin (Levels (**I**) and (**II**) in Fig. 1) are obtained via *ab initio* calculations using Density Functional Theory. The clusters of chitin-protein nanofibrils

(Level (**III**) in Fig. 1) are modeled as a long-fiber composite where the aligned chitin nanofibrils are embedded in a protein matrix. The homogenized properties of this composite are found with a Mori-Tanaka homogenization scheme [3] and taken to be the effective properties of a single chitin-protein fiber (Level (**IV**) in Fig. 1). The Bouligand plywood structure with a system of pore canals (Fig. 1, Level **VI**) is modeled as 3 identical families of fibers rotated at 60° w.r.t. each other. The pore canal system (Level (**V**) in Fig. 1) is taken into account as an array of hexagonal holes piercing the homogenized cuticle. The mineral-protein matrix in the bulk cuticle tissue is a composite assembly of calcium carbonate spheres embedded in a matrix of cuticle proteins. Its properties are found with a 3-point estimate [4].

3. Results

The model predictions are compared with experimental data for wet lobster cuticle.

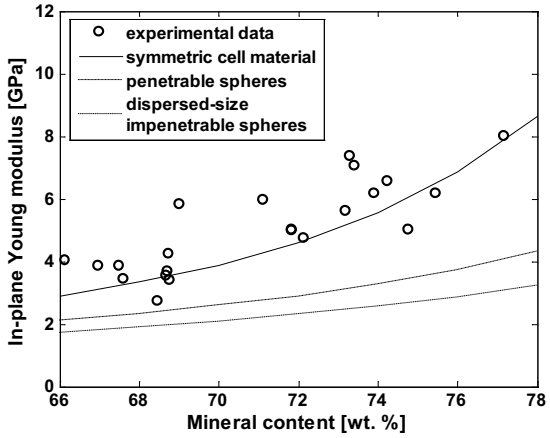

Figure 2. In-plane Young modulus of wet lobster endocuticle vs. mineral content. Lines: model predictions, open circles: experimental data.

In Fig. 2 we compare the predicted in-plane Young modulus for different spherical assemblies of the mineral-protein matrix with experimental data. Our simulations suggest that the only microstructure of the mineral-protein matrix that provides for the experimentally observed increase of the elastic modulus is that of a symmetric cell material. In Fig. 3, it is seen that the in-plane modulus is quite sensitive to the area fraction of the canals and increases when the area fraction decreases. Most of the scattering in the measured modulus can be explained by the biological variation of the area fraction of the cuticle canal pores.

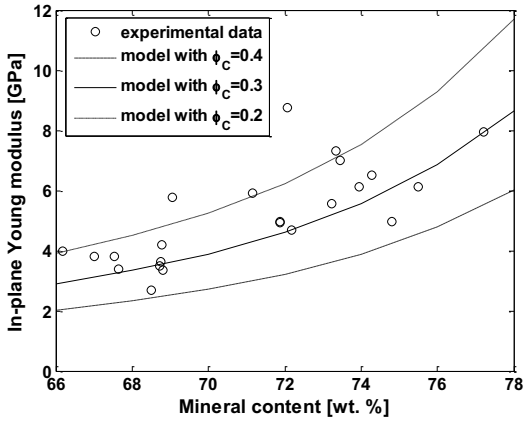

Figure 3. Influence of the area fraction of the canals ϕ_C on the in-plane Young modulus. Lines: model predictions, open circles: experimental data.

6. Conclusions

It is found that i) the mineral content; ii) the microstructure of the mineral-protein matrix and iii) the area fraction of the cuticle canal pores are the dominant factors that determine the overall cuticle stiffness. The cuticle stiffness increases significantly with increase in the mineral content and decreases with increase in the area fraction of the canals. The simultaneous variation in mineral content and area fraction of the canals can explain most of the scattering in the measured elastic moduli. Our results suggest that the microstructure of the mineralized tissue consists of amorphous calcium carbonate spheres with varying diameters forming a microstructure known as symmetric-cell material, which has extremal properties in terms of stiffness.

Acknowledgements

The authors gratefully acknowledge the financial support from the Gottfried-Wilhelm-Leibniz programme of the Deutsche Forschungsgemeinschaft (German Research Foundation).

References

[1] C. Sachs, H. Fabritius and D. Raabe, “Influence of Microstructure on Deformation Anisotropy of Mineralized Cuticle from the Lobster *Homarus Americanus*”, Journal of Structural Biology, **161,** 120 (2008).

[2] S. Nikolov and D. Raabe, “Hierarchical Modeling of the Elastic Properties of Bone at Submicron Scales: The Role of Extrafibrillar Mineralization”, Biophysical Journal, **94**, 4220 (2008).

[3] Y. Benveniste, “A New Approach to the Application of Mori-Tanaka's Theory in Composite Materials”, Mechanics of Materials, **6**, 147 (1987).

[4] S. Torquato, “Effective Stiffness Tensor of Composite Media: II. Applications to Isotropic dispersions”, Journal of the Mechanics and Physics of Solids, **35**, 1411 (1998).

Application of Computational Homogenization to the Deformation of Biological Tissue

Pieter Ghysels[1], Giovanni Samaey[1], Bert Tijkens[2], Paul Van Liedekerke[2], Herman Ramon[2], Dirk Roose[1]

[1]Department of Computer Science, K.U.Leuven, 3001 Leuven, Belgium
(E-mail: pieter.ghysels@cs.kuleuven.be)
[2]Department of Biosystems, K.U.Leuven, 3001 Leuven, Belgium

ABSTRACT

We present a multiscale method for the computation of large viscoelastic deformations of plant tissue, based on the concept of representative volume elements (RVEs) and similar to the approach presented in [1]. At the microscopic level, we use a discrete element model to describe the geometric structure and basic properties of onion epidermis tissue [2]. The macroscopic domain is discretized using standard finite elements, in which the unknown material properties (the stress-strain relation) are computed using the microscopic model in small subdomains (the RVEs). To these RVEs, a macroscopic deformation is applied via appropriate boundary conditions, and from the equilibrium solution, the corresponding Cauchy stress tensor is computed via a virial stress formula. The spatial elasticity tensor is estimated via forward differencing of the Truesdell rate of the Cauchy stress [3]. Viscoelastic behavior is simulated by applying not only macroscopic deformations but also a macroscopic velocity gradient to the RVEs. We focus on the consistent initialization of the RVE with both deformation and deformation velocity. For the use in an implicit timestepper we compute an approximation to the fourth order viscosity tensor by finite differencing, similar to the computation of the elasticity tensor. We demonstrate via numerical experiments that the resulting computational multiscale method converges to the solution of the full microscopic solution for successively refined meshes. We observe that by decoupling the full microscopic domain into many small microscopic simulations inside the RVEs, we can achieve a large speedup compared to a full microscopic simulation, this even when the separation in spatial scales is rather small.

[1] V. Kouznetsova, W. A. M. Brekelmans, and F. P. T. Baaijens, "An approach to micro-macro modeling of heterogeneous materials," Computational Mechanics, **27**, 37 (2001).
[2] J. Loodts, E. Tijskens, C. Wei, E. Vanstreels, B. Nicolai, and H. Ramon, "Micromechanics: Simulating the elastic behavior of onion epidermis tissue," Journal of Texture Studies, **37**, 16 (2006).
[3] C. Miehe, "Numerical computation of algorithmic (consistent) tangent moduli in large-strain computational inelasticity," Computer Methods in Applied Mechanics and Engineering, **134**, 223 (1996).

Direct Numerical Simulations for Electrokinetics of Colloids

Ryoichi Yamamoto[1], Takuya Iwashita[1] , Yasuya Nakayama[2] , Kang Kim[3]

[1]Kyoto University; [2]Kyushu University, Japan
[3]Institute for Molecular Science, Japan
(E-mail: ryoichi@cheme.kyoto-u.ac.jp)

ABSTRACT

We have developed a novel method for direct numerical simulations (DNS) of dense colloidal dispersions [1]. This method enables us to compute the time evolutions of colloidal particles, ions, and host fluids simultaneously by solving Newton, advection-diffusion, and Navier-Stokes equations so that the electro-hydrodynamic couplings can be fully taken into account. The electrophoretic mobilities of charged spherical particles are calculated in several situations. The comparisons with approximation theories show quantitative agreements for dilute dispersions without any empirical parameters; however, our simulation predicts notable deviations in the case of dense dispersions [2]. Recently, there observed experimentally the formation of string-like objects made of charged colloidal particles, similar to a "pearl chain" if external AC electric fields are applied. We have used our numerical method to investigate the mechanisms of this phenomena. We calculated the force acting between a pair of particles fixed at a constant distance r with and without external AC fields. Distributions of ions become anisotropic under electric fields. This leads to an occurrence of anisotropic dipole-dipole type interactions which can be a possible mechanism for the pearl chain formation.

[1] KAPSEL Homepage, http://www-tph.cheme.kyoto-u.ac.jp/kapsel/
[2] Kim, K., Nakayama., Y, and Yamamoto, R., Phys. Rev. Lett. 96, 208306, (2006).

Computer Design of Water Vapor Nucleation Rate Surface

Lyubov Anisimova[1], Michael P. Anisimov[2], and Philip K. Hopke[3]

[1]Department of Physics, Binghamton University, SUNY, Binghamton, NY 13903, USA
[2]Institute of Chemical Kinetics and Combustion SB RAS, Novosibirsk 630090, Russia
[3]Department of Chemical & Biomolecular Engineering, Clarkson University, Potsdam, NY 13699, USA (E-mail: [2]anisimovmp@mail.ru)

ABSTRACT

Nanomaterials can be produced as a result of nucleation. Computer modeling of nanoparticle generation typically employs some form of nucleation theory. However, given the problems with existing theories, this approach often has poor reliability. A semiempirical algorithm has been developed to compute embryo formation kinetics using water as an example. Such an approach to the design of the nucleation rate surface produces much higher data reliability since it is based on what is known regarding nucleation rates for the system of interest.

1. Introduction

Nucleation is the first stage for nanomaterial design. Computer modelling of nanoparticle generation is based on some form of nucleation theory. During the previous century, classical nucleation theory (CNT) was developed. Summarizing the state of nucleation theory, it can be concluded that theory is far from complete. It may be possible to successfully describe nucleation using simple models of considerably simplified real systems [1-3], but typically fails to fully reflect the nucleation behaviour over a wide range of nucleation conditions. Thus, experimental measurements are still the best source of the information on nucleation. A computer algorithm for semiempirical design of nucleation rate surfaces has been developed using the water vapor-droplet formation as an example.

2. Basic Principles

The nucleation rate surface for any system can be constructed over its phase diagram [4]. The concept involves using the phase equilibrium diagram to establish lines of zero nucleation rates. Nucleation rate surfaces arise from the equilibria lines. Only limited experimental data needs to be available to permit normalization of the slopes of the linearized nucleation rate surfaces. The following assumptions are applied. (1) A given phase can exist beyond its interphase equilibrium conditions. An interface equilibria line exists in the area of the other stable phase representing unstable equilibria of the parent phases. (2) The state diagram lines for the interphase equilibria represent lines of zero nucleation rates for the phases in equilibrium. (3) The highest nucleation rate for a given constant pressure or temperature is obtained at the

spinodal decomposition line. (4) For simplicity, the spinodal vapor pressure is taken to be the same for the formation of both the liquid and crystal phases. Most of these assumptions are commonly used to describe first order phase transitions. Systems cannot reach the conditions of the second order phase transition because of the growing fluctuations near the phase transition in the parent phase. Neither liquid (glassy) nor crystal phases have a zero probability of formation [5] for the available vapor supersaturation at temperatures lower than point *a* in Fig. 1.

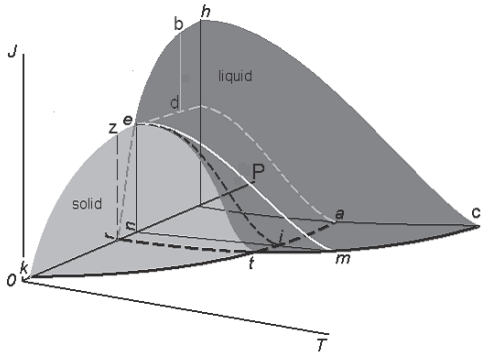

Fig. 1. Nucleation rate (J) surfaces for crystal and droplet formation in the vicinity of triple point. T and P are temperature and total pressure respectively.

To frame the issues to be presented below, the key findings of Anisimova *at al.* [5] are briefly reproduced here. Figure 1 schematically illustrates the nucleation rate surface topology for a system with a triple point. For more details, see Anisimov and Hopke [6]. Lines *kt* and *tm*c illustrate the vapor–crystal and vapor-liquid equilibrium lines, respectively. Points *t* and *c* are the triple and critical points respectively. The lines of interphase equilibria can be continued through the triple point to a region of unstable equilibrium. The vapor-crystal equilibria line *kt* can be continued to point *a*, placed on the line of the vapor spinodal decomposition in the *PT* plane. The vapor-liquid line of equilibria, *tmc*, is continued to the region of the equilibrium crystalline phase (dotted extension for line *tmc* in Figure 1). Following the assumptions given above, the nucleation rate along the stable and unstable equilibrium lines is zero. The highest nucleation rates occur over the line of the spinodal decomposition. Nucleation rate surfaces can be drawn between the zero and highest nucleation rate lines. The nucleation rate surface for droplets, including glassy particles is shown by the dark gray color. The hidden part is shown by contour *ter*. The light gray color surface and its hidden extension represent the nucleation rate surface for the crystalline phase. The surface for crystal formation penetrates through the droplet surface. The kinetic limitations for crystal embryo growth at high enough vapor supersaturation make the probability (and rate) of crystal formation lower than the glassy embryo rate. Near and at the spinodal decomposition conditions, the more highly structured crystal particles have kinetic restrictions and accordingly lower formation probability in comparison with less structured droplets. In order to obtain the total nucleation rates, the rates for droplets and for crystal particles as shown schematically in Figure 1 should be summed. At a constant temperature, Figure 1 shows the crystal nucleation rate, represented in part by line *ke*. Line, *eh*, corresponds to the droplet nucleation rate. Point *e* schematically illustrates the condition where the droplets and crystalline particle nucleation rates are equal. Two nucleation rate surfaces cross in the line of intersection, *et*, where the nucleation rates for droplets and crystals are equal. At a constant pressure as shown in Figure 1 by line *nm*, the nucleation rate surfaces at this

pressure can be traced to obtain intersection lines *em* and *ei*. The first, *em*, corresponds to the nucleation rate for droplets and the other to the formation rate of crystal embryos. The behavior of nucleation rates shown schematically in Fig. 1 is very similar to the experimentally observed size distributions by Anisimova *et al.* [5]. Figure 1 can be used as a guide for the semi-empirical nucleation rate surface design for nucleation in the vicinity of triple point.

3. Essential data to design the nucleation rate surface

The experimental separation of the vapor nucleation rates though two different channels of nucleation (ice and droplets in the present case) is a problem for future research. The separation into two-channel nucleation can be based on using a reasonable connection of the line of intersection of the nucleation surfaces for ice and droplets at the triple point. The experimental nucleation rates for droplets and crystal embryos intersect for the conditions of the experimental measurements [7]. Data for water nucleation rates [7] have been split schematically into two sets of data for vapor-crystal and vapor-liquid water nucleation. It should be noted that intersection of these nucleation rate surfaces in *JTP* and *JTS* axes do not coincide except at the triple point that is common to both lines. Here *S* is vapor supersaturation ratio. It is assumed that supersaturation for the experimental data is ratio of the actual and solid vapor pressures.

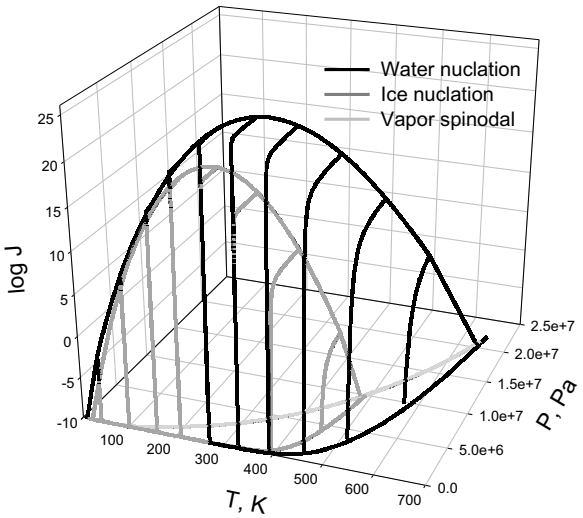

Fig. 2. Nucleation rate surfaces for water droplets and ice formation in the log *J-P-T* axes.

Approximations of the experimental nucleation rates, $J_{T(K)}$, are then used for the associated nucleation temperatures, *T*(K), as functions of the vapor supersaturation, *S* as well: $\log J_{220} = 20.7985 - 22.6027/\log^2 S$; $\log J_{230} = 22.4170 - 20.5603/\log^2 S$; $\log J_{240} = 23.4185 - 17.8059/\log^2 S$; $\log J_{250} = 23.3452 - 14.5839/\log^2 S$; $\log J_{260} = 22.4477 - 11.2255/\log^2 S$. It was assumed that the nucleation rates can be represented by these linear approximations for both phases over all possible conditions. To semi-empirically design the nucleation rate surface, it is necessary to have: (1) Equilibrium phase data including the unstable equilibria. (2) The equations of state for system under consideration. (3) Experimental data on nucleation rates for each channel of nucleation. (4) An algorithm for the extrapolation of experimental nucleation rate to the spinodal and to zero nucleation rate conditions. The equation of states used is $P = RT/(V-b) - aV^{-2}$,

where V is volume; R is gas constant; $a = 27(RT_c)^2/64P_c$ and $b = RT_c/8P_c$. The critical temperature, T_c = 647.3 K, and the critical pressure, P_c = 22.04832 MPa, for water are taken from Handbook of Chemistry and Physics. Spinodal conditions were extrapolated from 220 K to the absolute zero temperature using equation $\log P_{sp} = 7.2159 - 217.5720/T$. Fig. 2 illustrates the resulting topology of the water vapor nucleation rates.

4. Summary

This study is designed to help clarify several important issues in nucleation using a computer model of the nucleation rate surface such as that for water vapor supersaturation and nucleation rates at the spinodal conditions. Water vapor equilibrium and spinodal conditions were obtained by extrapolation of the handbook data for vapor equilibria and data for spinodal conditions extracted from the Van der Waals equation of state. An algorithm for modeling of the nucleation rate surfaces for the full field of the nucleation parameters was developed. A simplified nucleation rate surface for water vapor nucleation was designed. The phase transitions in ice are not taken it to account to make the illustration simpler. This example illustrates the clear promise for the use of the semi-empirical construction of the nucleation rate surfaces. It may be possible to simplify the experimental measurements as a result of optimizing (by minimization of number of experimental points) the empirical data collection and using measurements for easily available experimental conditions. An obvious advantage of the semi-empirical construction of nucleation rate surfaces is the ability to design this surface over the full interval of nucleation parameters that are unavailable for laboratory experiments. Examples of conditions that are difficult to achieve include very low temperatures, high-pressures, and/or very high-temperature medium (stars) *etc*. It is assumed that the current algorithm can be further developed for the semi-empirical design of nucleation rate surfaces for one- and two-component systems.

4. Acknowledgements

Research is under support of the Russian Foundation for Basic Research through grant numbers of 07-08-13529-ofi and 07-03-00587-a.

References

[1] H. Reiss, in *Nucleation and Atmospheric Aerosols*, Edited by B. Hale and M. Kulmala (AIP, Melville, NY, 2000) p. 181.
[2] V. Kalikmanov and M. E. H. van Dongen, J. Chem. Phys., **103**, 4250 (1995).
[3] R. McGrow, in *Nucleation and Atmospheric Aerosols*, Edited by B. Hale and M. Kulmala (AIP, Melville, NY, 2000) p. 373.
[4] M.P. Anisimov, P.K. Hopke, D.H. Rasmussen, S.D. Shandakov, V.A. Pinaev, J. Chem. Phys. **109**(4), 1435 (1998).
[5] L. Anisimova, P.K. Hopke, and J. Terry, J. Chem. Phys. **114**, 9852 (2001).
[6] M.P. Anisimov, P.K. Hopke, J. Phys. Chem. B **105**, 11817 (2001).
[7] Y. Viisanen, R. Strey, and H. Reiss, J. Chem. Phys. **112**, 8205 (2000).

Simulations of Electronic Properties of Self Assembled Soft Materials: DNA-adsorbents and Amorphous Polyfluorenes

Svetlana Kilina, Segei Tretiak , Dzmitry Yarotski , Alexander Balatsky

Los Alamos National Laboratory, Los Alamos, New Mexico, USA
(E-mail: skilina@gmail.com)

ABSTRACT

The idea of harnessing the molecular building blocks to assemble nanometer-scale devices promises the fascinating applications ranging from electronic to medical ones. Advances in atomic-scale experimental imagining and manipulation techniques, e.g., STM, AFM, lithography, and ultrafast spectroscopy, pave the way to control the transport in such electronic devices, where all elements are parts of a single molecular-macro-assembly. Yet, the fundamental understanding of the underlying physics and chemistry of such complex structures lag the experiments. We use a combination of ab initio techniques, such as Density Functional Theory, with classical force field calculations to predict and to explain experimental results on transport properties of several molecular composites and disordered materials. Among the considered systems are: i) Adsorbed DNA strands on metallic surfaces. Here the unique STM spectra of bases promise fast sequencing of DNA. To interpret experimental results, we simulate tunneling spectra and identify the underlying electronic features of each DNA bases adsorbed on Cu(111) surface. Our simulations reveal that cytosine and guanine, having large dipole moments, interact strongly with the substrate through chemisorption, while thymine and adenine, having smaller dipole moments, are weakly physisorbed. The observed diversity of the geometrical and electronic structures of the nucleobases on the Cu substrate provides guidelines for interpreting DNA tunneling microscopy spectra, and shows perfect agreement between simulations and STM measurements. ii) DNA strands wrapped around carbon nanotubes (CNT). We focus on structural relaxation of DNA molecules in a presence of a CNT. Simulated structures coincide with recently resolved STM images of these systems. iii) Amorphous conjugated polymers, e.g. polyfluorenes (PFO). We have found that electronic and optical properties of this system are affected by disorder in torsion angles and in intra-chain conformational changes: the electron traps are induced by changes in intra-chain configuration, while hole traps originate from inter-chain correlations. Our quantum-classical numerical approach allows to describe extended complex systems on a quantum mechanical level and opens a new prospective for understanding of transport properties in bio- and conjugated polymers, interacting with each other or with inorganic substrates.

Self-diffusion in Binary Blends of Cyclic and Linear Polymers

Sachin Shanbhag

School of Computational Science, Florida State University, Tallahassee, FL, USA
(E-mail: shane5ul@gmail.com)

ABSTRACT

A lattice model is used to estimate the self-diffusivity of entangled cyclic and linear polymers in blends of varying compositions. To interpret simulation results, we suggest a minimal constraint release model for the motion of a cyclic polymer infiltrated by neighboring linear chains. Both, the simulation, and recently reported experimental data on entangled DNA solutions support the simple model over a wide range of blend compositions, concentrations, and molecular weights

Hydrophilic pore formation in lipid bilayers in the presence of edge-active agents: An atomistic simulation study

Raghava Alapati, Ram Devireddy, Dorel Moldovan

Department of Mechanical Engineering, Louisiana State University
(E-mails: ralapa1@lsu.edu, devireddy@me.lsu.edu, moldovan@me.lsu.edu)

ABSTRACT

We report molecular dynamics simulation studies that delineate, with atomistic details, the entropy-driven nucleation and growth of hydrophilic pores in lipid bilayers in the presence of an edge-active agent. Zwitterionic dimyristoylphosphatidylcholine (DMPC) lipid bilayer was chosen as the model membrane. As edge-active agent we used dimethylsulfoxide (DMSO), one of the most widely used solvents in cell biology and cryopreservation. Our simulations show that when the line tension of the DMPC bilayer is lowered by the presence of DMSO below a certain threshold, pores can be thermally nucleated and grow over atomistically accessible timescales. We rationalize the nucleation and growth process in terms of a simplified free energy model that includes the entropy of the pore shape. By estimating the line tensions within the lipid bilayers with and without edge-active agents, our simulations corroborate a pore growth model

Multiscale Simulation for Rheological Phenomena

Takahiro Murashima[1] and Takashi Taniguchi [2, 1]

[1]Core Research for Evolutional Science and Technology, Japan Science and Technology Agency Corporation, Kawaguchi, Saitama 332-0012, Japan;
[2]Graduate School of Science and Engineering, Yamagata University,
4-3-16 Jonan, Yonezawa, Yamagata 992-8510, Japan,
(E-mail: murasima@yz.yamagata-u.ac.jp)

ABSTRACT

We investigate multiscale simulation method based on Lagrangian particle methods and then find that the conventional Lagrangian particle methods are not suitable for multiscale simulations except for modified smoothed particle hydrodynamics (MSPH) which highly improves the original SPH. We incorporate MSPH with stochastic coarse-grained polymer simulators and show some typical example.

1. Introduction

In order to predict behaviors of polymeric liquids, it is quite important to know how to incorporate microscopic degrees of freedom of them to equations of macroscopic variables such a stress field. When we solve macroscopic equations, we need to use a constitutive equation that gives a relation between the stress field and velocity field. However, there is no general constitutive equation which is applicable to various soft matter systems because the stress field depends on complex entanglements between polymers. In order to solve the polymeric fluid macroscopically we choose the Lagrangian methods, e.g. Smoothed Particle Hydrodynamics (SPH) method [1] and Moving Particle Semi-implicit (MPS) method [2], since they have possibilities to treat fluid particles having internal degrees of freedom and conserving their history-dependent information, or polymers are disentangled or not. Of course, SPH and MPS can be applicable to non-Newtonian fluids by using the constitutive equations [3, 4] although their stress fields are defined between calculation points. Unfortunately these conventional Lagrangian methods are not practical to apply to multiscale simulations as it is because we cannot make one-to-one correspondence between macroscopic and microscopic stress fields.

Recently Zhang and Batra [5] have developed “Modified Smoothed Particle Hydrodynamics (MSPH)”. This method highly improves the original SPH method since the procedure to obtain first order derivative of physical quantities is based on a sort of deconvolution. By using MSPH, we can treat the stress tensors which are defined just on the calculating points not between two calculating points.

We explain our multiscale simulation method, which is MSPH with coarse-grained stochastic simulators incorporated into all each fluid particles, and show a typical example.

2. Macroscopic Simulation (Modified Smoothed Particle Hydrodynamics)

When we solve the differential equations, we need to know at least first order derivative of physical quantities. In terms of SPH, the first order derivative is as follows:

$$\langle \nabla f(\mathbf{r}_i) \rangle = \int_{\Omega} d\mathbf{r}_j \; f(\mathbf{r}_j) \nabla W(\mathbf{r}_j - \mathbf{r}_i), \tag{1}$$

where $f(\mathbf{r})$ is some physical quantity depends on the coodinates $\mathbf{r}$ and $W(\mathbf{r}) \sim e^{-r^2/h^2}$ is a gaussian kernel function.Of course, Eqn. (1) is not equal to $\nabla f(\mathbf{r})$. If we take this first order derivative twice in order to obtain the second order derivative, we lead a wrong result. Espetially near surface boundaries, the result causes unphysical oscillation when we solve diffusive type differential equations including the Navier-Stokes equation.

MSPH method overcomes the above difficulty. This method is similar to the deconvolution procedure, and therefore it is somewhat cumbersome. The result is highly improved rather than original SPH method since the first derivative of physical quantity obtained with MSPH is $\nabla f(\mathbf{r}) + O(\Delta^3)$ where Δ is initial distance between fluid particles. MSPH is abbreviated to solve the next linear equations:

$$\mathbf{A}\mathbf{x} = \mathbf{b}. \tag{2}$$

Each components of Eqn. (2) consist of the following equations:

$$A_{IJ} = \int_{\Omega} d\mathbf{r}_j \; R_I K_J, \qquad (\{I, J\} = \{1, \cdots, 10\}) \tag{3}$$

$$\mathbf{x} = \left\{ f_i \; f_{i,x} \; f_{i,y} \; f_{i,z} \; f_{i,xx} \; f_{i,yy} \; f_{i,zz} \; f_{i,xy} \; f_{i,yz} \; f_{i,zx} \right\}^T, \tag{4}$$

$$b_I = \int_{\Omega} d\mathbf{r}_j \; f_j K_I, \tag{5}$$

$$\mathbf{R} = \left\{ 1 \; r_x \; r_y \; r_z \; \frac{r_x r_x}{2} \; \frac{r_y r_y}{2} \; \frac{r_z r_z}{2} \; r_x r_y \; r_y r_z \; r_z r_x \right\}^T, \tag{6}$$

$$\mathbf{K} = \left\{ W_{ij} \; W_{ij,x} \; W_{ij,y} \; W_{ij,z} \; W_{ij,xx} \; W_{ij,yy} \; W_{ij,zz} \; W_{ij,xy} \; W_{ij,yz} \; W_{ij,zx} \right\}^T, \tag{7}$$

$$r_\gamma = \gamma_j - \gamma_i \quad (\gamma = \{x, y, z\}), \tag{8}$$

where $f_i = f(r_i)$ and $W_{ij} = W(r_j - r_i)$. Although we obtain not only f(r) but also f(r) from Eqn. (4), we don't use the latter one here.

3. Microscopic Simulation (Stochastic Dumbbell Model)

Our multiscale simulation is similar to CONNFFESSIT (Calculation of Non-Newtonian Flow: Finite Elements and Stochastic Simulation Technique) [6], which is communicating through deformation velocity fields (macro to micro) and stress fields (micro to macro). Here we adopt Hookean dumbbell model as microscopic polymer simulator:

$$dQ = \left(\kappa \cdot Q - \frac{1}{2\tau}Q\right)dt + \sqrt{\frac{dt}{\tau}}\Phi, \tag{9}$$

where $\kappa = (\nabla v)^T$, Q is end-to-end vector, and τ is relaxation time of dumbbells. Φ is Gaussian vector satisfying $\langle\Phi(t)\rangle = 0$ and $\langle\Phi(t)\Phi(t')^T\rangle = I\delta(t-t')$. Here we numerically integrate Eqn. (9) by using the stochastic Runge-Kutta algorithm [7]. Macroscopic stress is expressed as the second moment of the configuration distribution function:

$$\sigma^p = \frac{\eta_p}{\tau}(-I + \langle QQ\rangle), \tag{10}$$

where η_p is the polymeric viscosity. Note that Eqn. (9) and Eqn. (10) are appropriately normalized. The Hookean dumbbell model corresponds to the upper-convected Maxwell model [8]:

$$\dot{\sigma^p} - \kappa \cdot \sigma^p - \sigma^p \cdot \kappa^T + \frac{1}{\tau}(\sigma^p - GI) = 0, \quad G = \eta_p/\tau. \tag{11}$$

Figure 1 shows the time evolution of the stress tensor under constant strain rate, comparing the stochastic dumbbell model with the upper-convected Maxwell model.

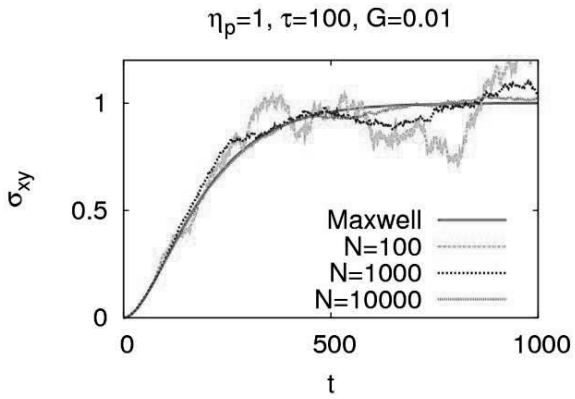

Figure.1: Comparison of the Hookean dumbbell model (different numbers of dumbbells) and the upper-convected Maxwell model. The longitudinal axis represents the stress tensor σ_{xy} and the transverse axis shows the time t.

4. Multiscale Simulation (Primary Plane Flow Problem)

Here we show multiscale simulation results applying to the primary flow problem between parallel plane plates. Each fluid particle has $N = 1000$ dumbbells simulating polymer dynamics.

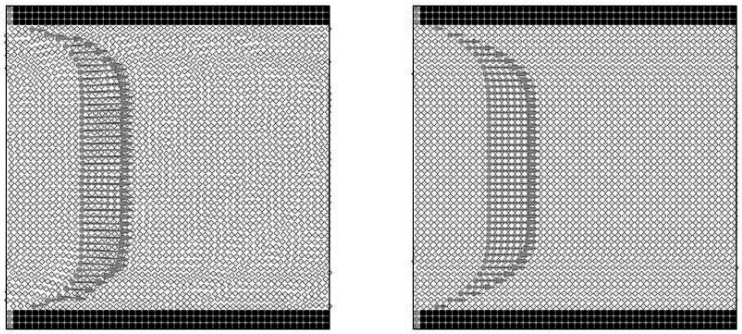

Figure 2: The left figure shows the startup flow simulated with the multiscale method (MSPH and the stochastic dumbbell model) and the right figure shows the usual macroscopic simulation (MSPH and the upper-convected Maxwell model).

5. Conclusion

We have proposed the new multiscale simulation incorporating the Lagrangian fluid dynamics with the stochastic polymer simulators and found that this method works well. Here we have adopted the artificial problem as a test case of our multiscale simulation. We expect that more realistic micro simulator will upgrade our method and then we can deal with practical issues.

References

[1] J. J. Monaghan, "Smoothed Particle Hydrodynamics", Reports on Progress in Physics, **68,** 1703 (2005).
[2] S. Koshizuka, "Moving Particle Semi-implicit method for fragmentation of incompressible fluid", Nuclear Science and Engineering, **123,** 421 (1996).
[3] M. Ellero, M. Kröger and S. Hess, "Viscoelastic flows studied by smoothed particle dynamics", Journal of Non-Newtonian Fluid Mechanics, **105,** 35 (2002)
[4] H. Nishitani and M. Doi "Biorheo Simulator VINE User's Manual (Japanese)" (2007).
[5] G. M. Zhang and R. C. Batra, "Modified smoothed particle hydrodynamics method and its application to transient problems", Computational Mechanics, **34,** 137 (2004).
[6] H. C. Öttinger "Stochastic Processes in Polymeric Fluids", Springer (1996)
[7] A.C. Branka and D. M. Heyes, "Algorithms for Brownian dynamics simulation", Physical Review E, **58,** 2611 (1998)
[8] R. G. Larson "The Structure and Rheology of Complex Fluids", Oxford University Press (1999)

Modeling of Biofilm-Flow Interaction Using Kinetic Theories

Qi Wang, Tiangyu Zhang

Department of Mathematics, Florida State University, Tallahassee, FL -32306
(E-mail: wang@math.fsu.edu)

ABSTRACT

We present a kinetic model for biofilm-solvent mixture accounting for the microstructure of the extracelluar polymer substances in biofilms. At the coarse-grain level approximation, it leads to a phase field model for biofilm-solvent mixture. Two distincitive growth modes can be identified. Bacterial, disinfectants, and other significant components in the biofilm can be modeled as desired. Numerical simulation of the biofilm dynamics will be presented.

A Molecular Simulation Study on Gas Transportation in Ploy(chloro-para-xylene)) Membrane

Chunhai Lu[1], Shijun Ni[2] , Wenkai Chen[3] , Chengjiang Zhang[2]

[1]China Academy of Engineering Physics, P.O. Box 919-71, Mianyang, PR China
[2]Chengdu University of Technology, Chengdu, PR China
3 Department of Chemistry, Fuzhou University, Fuzhou, PR China
(E-mail: luchhi@126.com)

ABSTRACT

The aim for this research is to explore and investigate the diffusion of gases in ploy(chloro-para-xylene)) membrane. Results of molecular dynamics (MD) and Monte Carlo (MC)simulations on transport and solubility of small molecules such as helium, nitrogen, oxygen, water, carbon oxide in ploy(chloro-para-xylene)) membrane are discussed. Atomistic simulation techniques have proven to be a useful tool for the understanding of structure-property relationships of materials. Although MD and MC still not an ideal tool for quantitative prediction of gas permeation properties, these methodologies can be used for a detailed description of the complex morphologies and transport mechanisms associated with rigid glassy structures. The diffusion coefficients of gases are determined via NVT molecular dynamics simulation using COMPASS force field up to 400ps simulation time. The diffusion process results from jumps of penetrant molecules between adjacent holes in polymer matrix. the free volume and the occurring jump mechanism are characterized and visualized with different methods. Constants of diffusion and solubility coefficients have been calculated by Transition State Gusev-Suter Monte Carlo method revealing a considerable agreement between simulated and calculated data (fig.1 and fig.2). Fig.1 Simulated diffusion coefficients of gas molecules Fig.2 Simulated sorption isotherms of helium at 298K .

[1] Richard H. Boyd, P.V. Krishna Pant. Macromolecules. 1991, 24, 6325-6331
[2] H. Sun. J. Phys. Chem. B. 1998, 102, 7338-7364
[3] E. Tocci, d. Hofmann, D. Paul, N. Russo, E. Drioli. Polymer. 2001, 42, 521-533

Multi-Time Scale Deterministic and Stochastic Analysis of the Heat Shock Response System

Anke Meyer-Baese

Florida State University, Tallahassee, FL, USA
(E-mail: amb@eng.fsu.edu)

ABSTRACT

In many cellular systems the molecular populations of some reactant species are either very small or the dynamic structure of the system is prone to parameter variations and/or stochastic disturbances. This fact demonstrates the necessity of viewing both parametric uncertainty and stochasticity as an important aspect of modeling of biological systems. The heat shock response represents a such a system susceptible for molecular fluctuations. The heat shock is responsible for unfolding of proteins at the cellular level and thus affecting cellular function. The cells' response to it is based on the initiation of the production of heat-shock proteins (hsps) with the role of chaperones refolding denaturated proteins into their initial states, or proteases that degrade them. In the present paper, we are investigating the effect of uncertainties of feed back and feedforward parameters and several molecular fluctuations on the heat shock response. The goal is to study the dynamic stability properties of the bacterial heat stress response, modelled by a reduced-order system, from a rigorous analytic standpoint and to apply results of the theory of nonlinear mixed deterministic and stochastic singularly perturbed and uncertain systems. The system under study models the dynamics of both fast states such as the protein folding as a deterministic nonlinear singularly perturbed component and slow states such as the sigma-factor and chaperones as the stochastic nonlinear singularly perturbed components. As a result of the stability analysis, we obtain upper bounds for the time constant of the fast system, for the autocorrelation and variance of the stochastic fluctuations and domains for system's parameters for achieving robust stability.

A Study on Application of Underwater Shock Wave for Jute Fiber Processing.

G.M.Shafiur Rahman[1], Shigeru Itoh[2]

[1]Graduate school of Science and Technology, Kumamoto University, Japan
[2]Shock Wave and Condensed Matter Research Center, Kumamoto University
2-39-1 Kurokami, Kumamoto 860-8555, Japan.
(E-mail: gmsrahman@yahoo.com)

ABSTRACT

Jute (Corchorus Olitorious) second most important natural fiber after cotton. It is the golden fiber of Bangladesh and at present, it is the third foreign currency earner next to the garments and manpower sectors. There are about 80 jute mills in Bangladesh. But they are using conventional jute processing method and producing conventional jute products. Jute also has the ability to blend with other fibers, both synthetic and natural fiber. As the demand for natural biodegradable comfort fiber increases, the demand for jute and other natural fibers that can be blended with cotton increase. To meet this demand and to get improved properties it should modernize processing of jute. In this investigation, we have developed an underwater shock wave technique to treat the jute fiber for the improvement its properties by inducing micro cracks or pores on the surface of jute fiber. To make the process efficient, the optimum underwater shock wave technique by using explosion was established on the basis of different parameters such as explosive, pressure or shock strength, detonator height (Dh), polyethylene paper thickness etc. After underwater shock wave treatment different characteristics of jute fiber such as moisture content, permeability (depending on time, dyeing temperature, shock strength, dye concentration) and SEM images have been investigated. Percentage of weight of damaged jute fiber after shock treatment due to explosion has been counted in the investigation. It has been seen that the percentage permeability or absorbance of dye of underwater shock treated jute fiber is higher than that of un-shock treated jute fiber. Flame resistance characteristic and breaking strength of jute fiber after and before shock treatment have also been studied

Umbrella Sampling Simulations of the Closure of Biotin Carboxylase

Brian R. Novak[1], Dorel Moldovan[1], Grover L. Waldrop[2], Marcio S. de Queiroz[1]

[1]Louisiana State University, Mechanical Engineering, Baton Rouge, LA 70803, USA
(E-mails: bnovak1@lsu.edu, dmoldo1@lsu.edu, mdeque1@lsu.edu);
[2]Louisiana State University, Biological Sciences, Baton Rouge, LA 70803, USA
(E-mail: gwaldro@lsu.edu)

ABSTRACT

Biotin carboxylase is a homodimer that utilizes ATP to carboxylate biotin. Solid state studies of the enzyme using x-ray crystallography revealed a prominent conformational change upon binding ATP. To determine the importance of this closing motion, the potential of mean force with the closure angle as a reaction coordinate was calculated using molecular dynamics simulations and umbrella sampling for a monomer of *E. coli* biotin carboxylase in water with restraints to simulate attachment to a surface. The result suggests that the most stable state for the enzyme is a closed state different from both the ATP bound and open state crystal structures. There is also a significant motion of a region near the dimer interface not predicted from the crystal structures which may have implications for the dynamics and activity of the dimer.

1. Introduction

The enzyme biotin carboxylase catalyzes the ATP dependent carboxylation of biotin. Although it is one component of the multienzyme complex acetyl-CoA carboxylase that catalyzes the first step in fatty acid synthesis, it is a separate protein in bacteria [1] and can function independently. *In vivo* it occurs as a homodimer with each monomer having a complete active site. However, it has been shown that mutation of the dimer interface can lead to monomer formation without significant loss of activity [2]. The monomer consists of three domains. The A and C domains interact to form a large, globular section of the protein. Connected to these is the smaller, flexible B or ATP grasp domain. In the crystal structure of unliganded *E. coli* biotin carboxylase, the B domain is in an open state (PDB code 1DV1). In contrast, in the structure of an inactive mutant form with ATP bound, the B domain is in the closed down position.

Even though an open structure forms in the solid phase, this structure may not be stable in solution. The goal of this study was to calculate, using umbrella sampling, the potential of mean force (PMF) of a monomer in solution with a closure angle as the reaction coordinate. This PMF indicates the relative stability of open and closed states of the enzyme and the size of barriers.

2. Simulation Details

A monomer of *E. coli* biotin carboxylase was simulated using GROMACS 3.3.2 [3] with the GROMOS 43a1 force field. The starting structure was the crystal structure closed down on ATP

(PDB code 1DV2) with the mutated residue changed back to the wild type [4] and the ATP removed. All protein bonds were constrained and a time step of 2.0 fs was used. Periodic boundaries and the SPC model [5] for water were used.

Preparation consisted of addition of internal waters, a steepest descent energy minimization, addition of 14137 water molecules and a sodium ion to offset the -1 charge on the protein, an additional steepest descent energy minimization, and equilibration. During energy minimization, the enzyme backbone was restrained. Initial equilibration consisted of several steps. These include three isobaric (1 bar) and isothermal (300 K) 100 ps simulations with position restraints on: (i) the backbone atoms, (ii) only the N and C terminal atoms, and (iii) eleven atoms of three residues to simulate attachment to a surface. These final restraints were used in all subsequent simulations. Volume was then averaged over a 25 ps run at constant temperature and pressure. Finally, a 6 ns simulation was run at constant volume and 300 K.

3. Results

The Floppy Inclusions and Rigid Substructure Topography (FIRST) [6] program was used to determine the relatively rigid regions of the enzyme. It was run with a hydrogen bond cutoff of -0.40 kcal/mol on fifty closed configurations taken every 10 ps from a 500 ps trajectory. The "rigid" regions that were conserved in all fifty runs yielded three domains. Two were helices in the B domain (see Fig 1) and the third one was in the A and C domains and is not indicated.

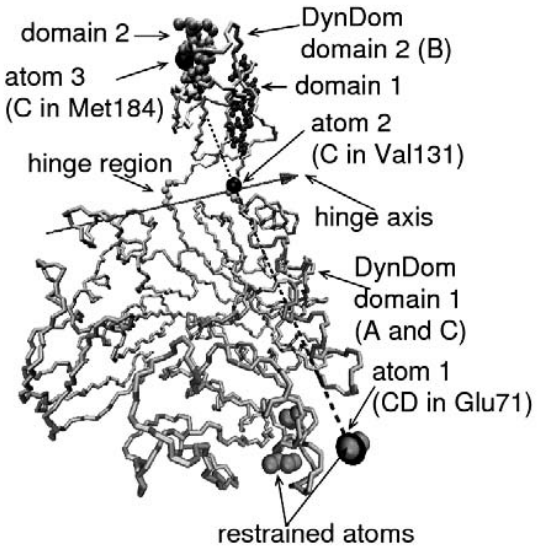

Figure 1. Domains, hinge regions, restrained atoms, and angle for umbrella sampling. The domains from FIRST are shown as blue and orange spheres. The backbone of the hinge residues (Cys130, Val131, Glu205, Asp206) from DynDom are shown as green spheres. The backbones of the domains from DynDom are shown in cyan and yellow, and the hinge axis is shown in purple. The restrained atoms are shown as red spheres, and the atoms used to define the angle are shown as black spheres connected by dashed lines and labeled as atoms 1 to 3.

DynDom [7] was run on open and closed configurations. Since the open crystal structure is missing electron density in the B domain, an open structure was generated from the closed one by pulling the closed structure open using steered molecular dynamics and equilibrating for 6 ns. The result of DynDom was two domains with a rotation angle of 46.5°, which is similar to the one obtained from crystal structures [4]. The rotation axis and hinge residues are shown in Fig 1.

The results from FIRST and DynDom were used to define an angle (θ) to use as the reaction coordinate for umbrella sampling. The angle was defined between an atom in domain 2, an atom in the hinge region, and one of the restrained atoms. Fig 1 shows the angle. The cosine angle restraint potential in GROMACS was used for the bias potentials.

Sixteen windows with equilibrium angles from 67° to 134° were used and the initial configuration for each window was taken from an adjacent one, except for the first one at 120°. Each initial configuration was equilibrated with its new bias potential before sampling.

Umbrella integration [8] was used to obtain the PMF shown in Fig 2(A). The global minimum corresponds to a closed state at θ = 71° and, at most, there are shallow minima for an open state that are about 10 kJ/mol above the global minimum. This means that before binding, the enzyme is in a closed state most of the time. The closed configuration is significantly different from the configuration with bound ATP (1DV2) since it leaves the binding site more open. See Fig 2(A).

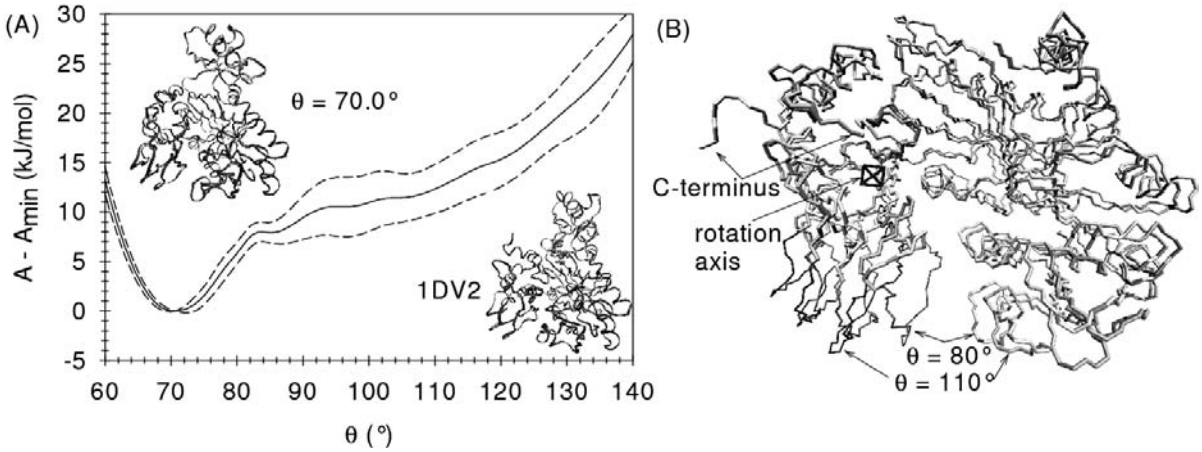

Figure 2. (A) A plot of the PMF difference. The reference is the global minimum at around θ = 71°. The solid line is the average of three 6 ns segments of data taken every 100 time steps. The dashed lines are two times the standard deviation of the mean away from the solid curve. The upper left inset is the enzyme backbone for the global minimum and the lower right one is 1DV2 with ATP in green. (B) DynDom analysis on DynDom domain 1 from Fig 1 for θ = 80° (green and blue) and 110° (yellow and red) from umbrella sampling simulations. The view is down the rotation axis shown as a black X. The blue region rotates 18° and the C-terminus changes location when θ goes from 80° to 110°.

Fig 2(B) shows a motion of DynDom domain 1 not predicted from the original DynDom analysis. The configurations in Fig 2(B) were taken from the umbrella sampling simulations, and DynDom was run on them to give a rotation of about 18°.

4. Conclusions and Future Directions

The results suggest that the open structure observed in the crystal structure of the unliganded enzyme is a consequence of the crystal contacts that atoms in the B-domain form with symmetry related molecules and not an inherent property of the protein. The lack of a significant energy minimum for an open state and a closed state global minimum that does not correspond to the structure with bound ATP raises two questions. Does the B domain open for substrate to enter or can ATP come in from the side of the closed conformation accompanied by a different conformational change? If the B domain opens, by how much? Answering these questions will be the subject of future investigation. Lastly, the motion shown in Figure 2(B) may be important for the dynamics and function of the dimer since it occurs near the subunit interface in the homodimer. Future work will simulate the dimer to help elucidate the communication mechanism between the monomers.

Acknowledgements

This work was supported in part by the LSU Innovation in Engineering Research Fund and the LSU Department of Mechanical Engineering.

References

[1] J.E. Cronan, Jr. and G.L. Waldrop, “Multi-subunit Acetyl-CoA Carboxylases”, Progress in Lipid Research, **41**, 407 (2002).
[2] Y. Shen, C.Y. Chou, G.G. Chang, and L. Tong, “Is Dimerization Required for the Catalytic Activity of Bacterial Biotin Carboxylase?”, Molecular Cell, **22,** 807 (2006).
[3] D. van der Spoel, E. Lindahl, B. Hess, G. Groenhof, A.E. Mark, and H.J.C. Berendsen, “GROMACS: Fast, Flexible, and Free”, Journal of Computational Chemistry, **26**, 1701 (2005).
[4] S.O.N. Lill, J.L. Gao, and G.L. Waldrop, “Molecular Dynamics Simulations of Biotin Carboxylase”, Journal of Physical Chemistry B, **112**, 3149 (2008).
[5] H.J.C. Berendsen, J.P.M. Postma, W.F. van Gunsteren, and J. Hermans, “Interaction Models for Water in Relation to Protein Hydration”, in *Intermolecular Forces*, edited by B. Pullman (D. Reidel Publishing Company, Dordrecht, 1981) 331-342.
[6] D.J. Jacobs, A.J. Rader, L.A. Kuhn, and M.F. Thorpe, “Protein Flexibility Predictions Using Graph Theory”, Proteins: Structure, Function, and Genetics, **44**, 150 (2001).
[7] S. Hayward and H.J.C. Berendsen, “Systematic Analysis of Domain Motions in Proteins from Conformational Change: New Results on Citrate Synthase and T4 Lysozyme”, Proteins: Structure, Function, and Genetics, **30,** 144 (1998).
[8] J. Kästner and W. Thiel, “Bridging the Gap Between Thermodynamic Integration and Umbrella Sampling Provides a Novel Analysis Method: "Umbrella Integration"”, Journal of Chemical Physics, **123**, 144104 (2005).